We would like to thank the editor for his very careful editing and constructive suggestions. In the following part, we make point-by-point responses to the comments and suggestions.

Thank you for responding to the reviewer's comments. I have 3 main concerns: 1) The manuscript is still not prepared for publication. There are numerous syntax problems that must be corrected, Many figures still need work, and figure 11 is missing!

Response: We appreciate the efforts the editor made to correct numerous syntax problems of our manuscript. We make all changes according to the suggestions.

2) Reviewer 2 asked you to investigate "how can you separate the effect of gravel on soil properties and other measured parameters" if the mudstoine bedrock is included in your soil pit samples and analysis. Again the question comes up as to how representative the site is.

Response: Thank you for your comments. Weathered mudstone is included in the sampling and analysis. It is not easy to separate the effects. Therefore, we used "coarse fragment soils", rather than gravel, throughout the manuscript.

We mentioned in Section 2.1 that:

"Based on the map of Li et al. (2015), soils of this region belong to Gelisols and Inceptisols, which occupy 34% and 28% of the total area of permafrost region of the QTP, respectively."

And in Section 4.1 that:

"The weight fraction of coarse fragment soil (diameter > 2mm, including gravel) in the soil samples we analyzed was greater than 55% on average. While the typical soil types considered in land surface models and other models usually have much smaller diameter. For comparison, the fractions of gravel considered in Pan et al. (2017) ranges from 5% to 33% and from 10% to 28% for the Madoi and Naqu sites, respectively. The Beiluhe site and the aforementioned sites are located in regions with Gelisols and Inceptisols, which occupy ~62% of the permafrost regions of the QTP (Li et al., 2015). It is possible that coarse fragment soil commonly exists on the QTP. The dataset of Wu and Nan (2016) indicated that gravel content widely exists on the middle and west part of the QTP."

Apart from these sources, we cannot assess the representativeness of the site.

3) Reviewer 2 thinks rightly so that your measured porosity is low because you did not use a vacuum to draw water through your sample (not weigh it under a vacuum condition). As a result, you will likely still have a fair amout of air. Rather than continue to have to deal with this as a nagging issue, I suggest that you run the simulations using calculated porosities. At the very least, discuss the differences in the two approaches.

Response: Thank you for your suggestion. We misunderstood the meaning of reviewer 2.

As mentioned in 2nd paragraph of Section 2.2, porosity is calculated based on equation 2, where weights of dry sample and saturated sample are used. The reviewer 2 mentioned that water of sample should be drawn under a vacuum condition, otherwise, there might be some water remained in the sample, and cause underestimation of porosity. However, sample was first dried in an oven for over 48 h, then weighed. Therefore, we believe that there might be a very low amount of water remained in the samples, especially for samples with poor water holding capacity (Figure 5).

As suggested, we add values of porosities derived from bulk density in Section 3.1.1, and discuss the uncertainties relating to porosity measurement in Section 4.3.1. We also made additional model simulations using the calculated porosities (Figure S6-S8).

Please see the

Section 3.1.1

"The porosity calculated from bulk density (= 1- bulk density/2.65 g cm-3) ranged from 29.8% to 39.2%."

Section 4.3.1

"It is ideal to draw water in soil samples under a vacuum condition before weighing dry soil sample. Unfortunately, we do not have such instrument. We dried soil samples in an oven at 65 ^{o}C for over 48 h, which is commonly used in ecological studies, e.g. Qin et al. (2018). The measured porosities are generally smaller than those calculated from bulk density. We made additional model simulations using porosities calculated from bulk density in combination with other measured parameters. Results showed that the RMSEs of ALD and PLB were 0.55 m and 4.78 m, respectively (Figures not shown). While those used measured porosities were 0.28 m and 6.71 m. Considering the importance of porosity on simulated permafrost dynamics, it is important to draw water out of soil samples before weighing dry soil samples in the future."

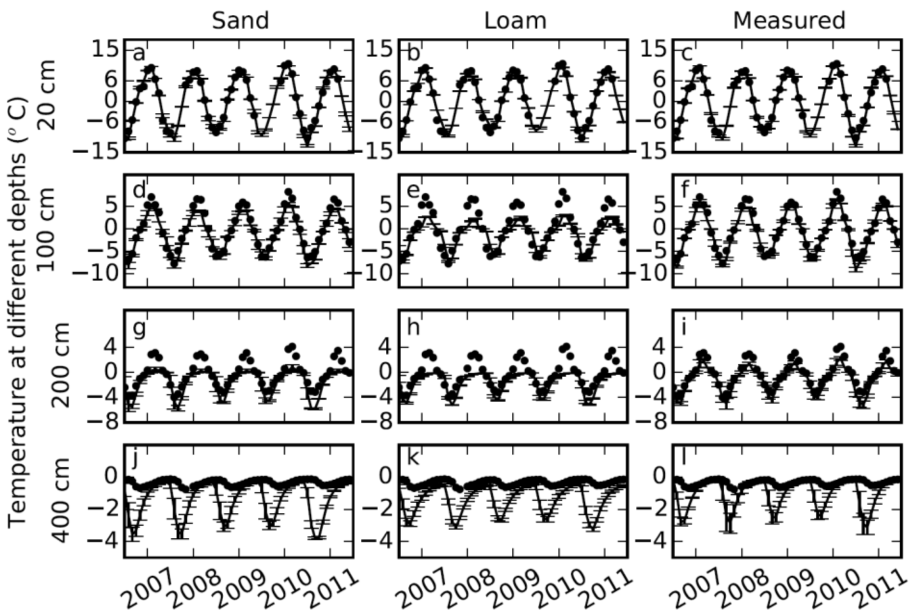

Figure S6. Comparisons of soil temperatures simulated using default parameters for sand, loam, and our measured parameters (lines) with measured soil temperatures (dots) at 20, 100, 200 and 400 cm depths. Error bars show the standard deviations calculated based on 9 simulations with 3 different slopes and 3 different soil thicknesses.(Calculated porosities from bulk density are used).

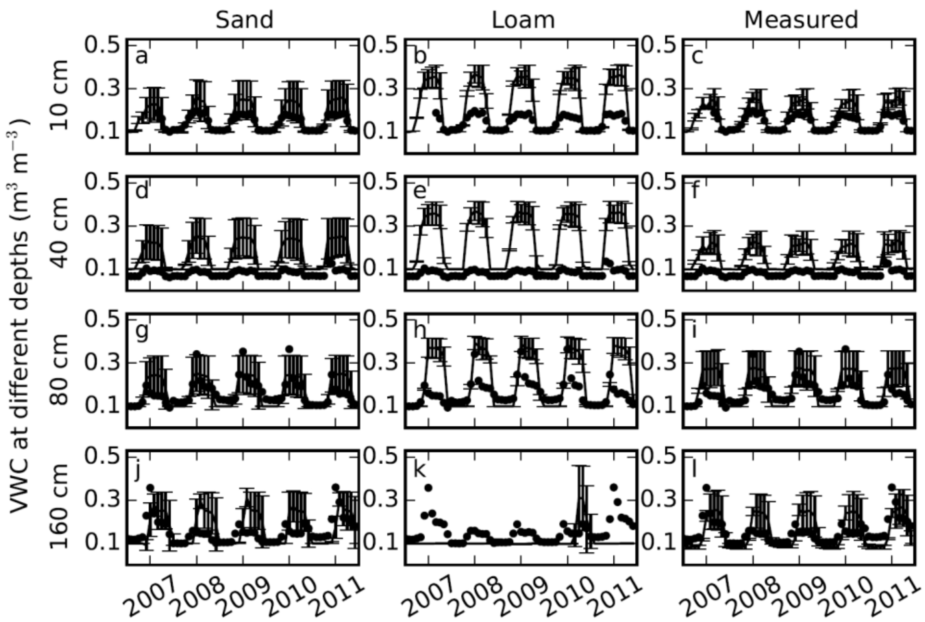

Figure S7. Comparisons of soil volumetric liquid water content (VWC) simulated using default parameters sand, default loam, and measured parameters (lines) with measured soil moistures (dots) at 10, 40, 80 and 160 cm depths. Error bars showed the standard deviation calculated based on 9 simulations with 3 different slopes and 3 different soil thicknesses (Calculated porosities from bulk density are used).

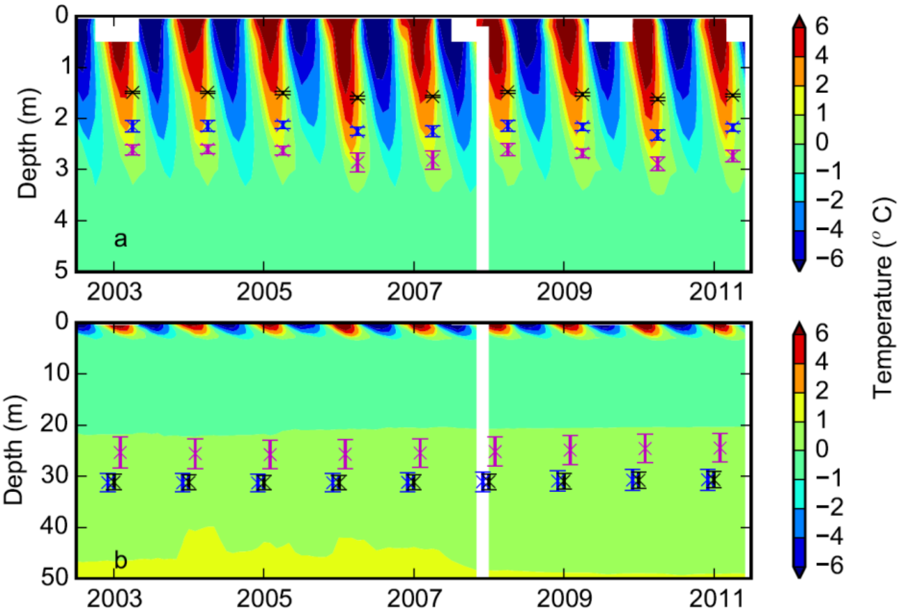

Figure S8. Contour plots showing a) soil temperature (°C) from borehole measurements down to 5 m superimposed with simulated active layer depths over the period of 2003-2011; and b) ground temperature down to 50 m superimposed with the simulated permafrost low boundary. Black, blue and magenta represent simulations with loam, sand and measured parameters, respectively. Error bars show the standard deviation calculated based on 9 simulations with 3 different slopes and 3 different soil thicknesses. (Calculated porosities from bulk density are used).

Page 4 Section 2.1 What is the depth to zero annual amplitude, and the temperature there? This paper could get cited just for that piece of information. Rather than 12 m, use the depth of zero annual amplitude because it yields MAGT (mean annual ground temperature).

Response: Thank you for your suggestion. We now include depth of zero annual amplitude and the multi-year annual mean temperature.

"Based on measurement, active layer depth is ~3.3 m, depth of zero annual amplitude is ~6.2 m, and the lower boundary of permafrost is at a depth of ~20 m.

The multi-year mean ground temperatures at 0.5, 6, and 60 m are about -0.52, -0.30 and 1.81 ^{o}C, respectively."

Page 6 Section 2.3 You don't day what permafrost dynamics you intend to model anywhere! It isn't until section 3.2 that we find out it is soil temp., liquid water, ALD, and PLB.

Response: Thank you for your comments. We now provide descriptions about the simulation of permafrost dynamics at end of Section 2.3.

"Soil temperatures, soil liquid water content, temperature in rock layers, active layer depth (ALD) and permafrost low boundary (PLB) were simulated explicitly."

Page 6 Section 2.3 It makes no sense to me why you rescale your 30 min interval data to monthly, and then downscale the monthly to daily time intervals. Soil temperatures in the model are updated daily. Simply use daily values determined from your 30 min data.

Response：Thank you for your comments. The family of TEM models is designed to simulate ecosystem dynamics over large regions. The monthly data from Climate Research Unit (CRU) is usually used as input. Daily data is downscaled within TEM to simulate environmental processes. Therefore, when we have daily or hourly dataset, we need to create monthly data first for driving model. We did not provide this explanation in the revised manuscript.

Page 7 Konard or Konrad. Check the spelling throughout the paper.

Response: Thank you for our comments. We used Konrad consistently throughout the manuscript.

Page 7 Follow this with some text about your assumptions regarding Tf and 0 deg. C.

Response: Thank you for your suggestion. We add description on the assumption.

"In DOS-TEM, freezing or thawing processes are assumed to be happened at Tf, following most of the land surface models (e.g. Oleson et al. 2010)."

Page 10 Please address R2's comment about measured versus calculated porosity here.

Response: Thank you for your suggestion. We include porosity which is calculated from bulk density. Table 1 is updated.

"The porosity calculated from bulk density (= 1- bulk density/2.65 g cm-3) ranged from 29.8% to 39.2%."

Page 10. Section 3.1.2 Give the threshold value here.

Response: Thank you for your suggestion. We include the threshold value in the text.

"The difference of saturated thermal conductivity between frozen and unfrozen states was about 0.85 W m-1 K-1. There existed a threshold of soil wetness (i.e. ~0.28 m^3 m^{-3}), below which frozen soil thermal conductivity was slightly smaller than unfrozen soil (Figure 4a)."

Page 14 Section 3.3.2. “Both 10 times？”

Response: Thank you for your comments. We modify the sentence to make the point clear.

"Among all the 18 cases with RMSEs less than the individual "best" RMSE, porosity was included 18 times, followed by thermal conductivity and hydraulic conductivity **both** with 10 times."

Page 16 Nowhere in the results do you mention permafrost degradation. See sections 3.2.3 and 3.2.4. You cannot say this.

Response: Thank you for your comments. We modify the sentence to make the point clear.

"As shown in this study, soil thermal and hydrological properties depend largely on soil water content."

Page 17 Delete. This is not related to the section heading, and is a distraction from the work in the paper.

Response: Thank you for your suggestion. We delete these sentences in the revised manuscript.

Page 18 This whole paragraph needs to be revised. You do not treat organic content, so that should be acknowledged, then go on to say why it was OK for you, but also why it should be looked into. The first sentence should be incorporated into the preceding paragraph.

Response：Thank you for your suggestion. We modify these sentences as suggested.

1) The first sentence is moved to the end of previous paragraph;
2) We acknowledge that we did not consider the organic content explicitly in this study and explain the reason

   "In the site considered in this study, the amount of organic soil carbon in soil was small (Figure 2), and we did not consider the effects of organic soil carbon on soil properties explicitly."

3) The reason why organic soil content should be considered has already explained in previous version of manuscript.

Page 19 Reference style is inconsistent. Follow a uniform style. Some references are in the wrong order. Please go over references carefully.

Response: Thank you for your suggestion. We go over the references carefully and make sure the style of references consistent and in right order.

Table 4 and 5

This is a mess and hard to read because of the line breaks. Figure out how to organize this table so that the substitutions are in line.

Response: Thank you for your suggestion. We now remove the "+" from the header of table.

Figures still need work

P31 Figure1:This image is blurry. Use a full resolution image ans include proper attribution to Google. I suggest saving the image from Google Earth that shows the attribution, then mark up the image with your locations and points. Save the image without compression. The image should be no less than 600 dpi

Response: Thank you for your suggestion. We do the work as suggested to save figure from Google Earth with attribution. However the image is blur (Please see Figure S1-1, we have problem of using Google Earth in China). We have to use third-part software to download high resolution image of Google Earth, but without attribution (Figure S1-2). In the modified manuscript, we use the high resolution image.

Figure S1-1. Image from Google Earth directly.

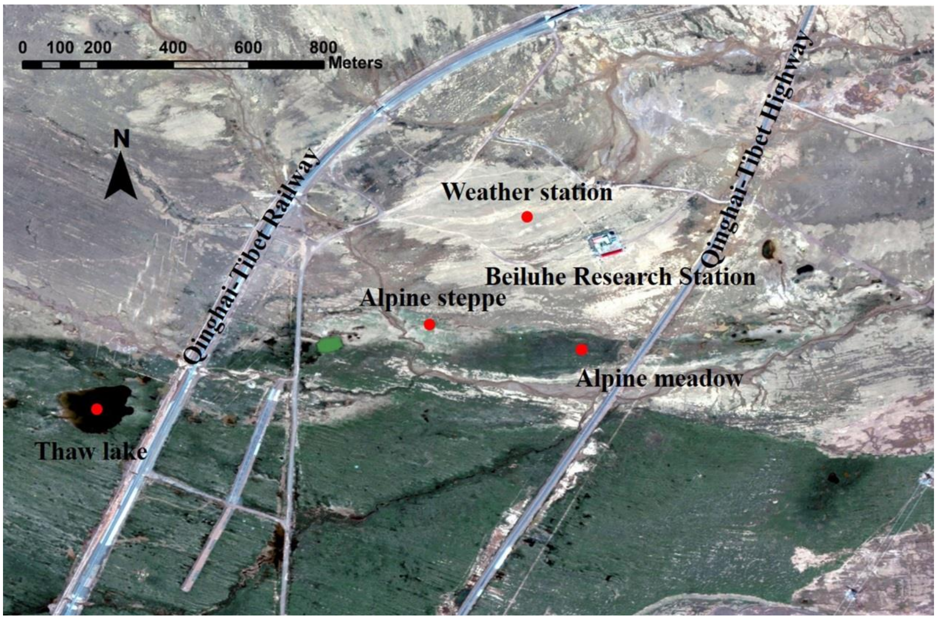

Figure S1-2. Image from third-part software.

P33 Figure3: Don't italicize.

Response: Thank you for your suggestion. We modified the figure as suggested.

P34 Figure4: unit (W m^{-1} K^{-1})

Response: Thank you for your suggestion. We modified the sentence as suggested.

P36 Figure 6: This plot is of temperature not depth. Re-label so that it is clear to the reader that the plots shows temperature

Response: Thank you for your comments. We now use "Temperature at different depth (°C).

P37 Figure 7:

1)Why are the depths shown different than Figure 6? For comparative purposes it would be best if they were the same, no?

Response: Thank you for your comments. Soil moistures were measured at depths of 5, 10, 20, 40, 80 and 160 cm (please see the 3rd paragraph of Section 2.1). However, we need to present the comparisons of soil temperature in the permafrost. In this site, the upper boundary of permafrost is about 3.3 m, therefore, we compare the simulated temperature down to 4 m.

2)This plot is of VWC not depth. Re-label so that it is clear to the reader that the plots shows VWC

Response: Thank you for your comments. We now use "VWC at different depth (m^3 m^{-3}).

P38 Figure 8: What are the white zones? Looks like an error. Please correct.

Response: Thank you for your comments. The white zones are caused by missing data of measured temperatures.

P38 Figure 8. No space between degree sign and C.

Response: Thank you for your comments. We plot our figures using python matplotlib. We specified "^{o}C", there is no space between o and C. However there seems a small space between them. We cannot remove the small space.

P39 Figure 9: Slope = 10^o

Response: Thank you for your suggestion. We modified the figure as suggested.

P41 Figure 11: Figure is clearly missing!

Response: Sorry for the mistake. We now add the figure in the main text.

The physical properties of coarse ~~soil~~ fragment soils and their effects on permafrost dynamics: A case study on the central Qinghai-Tibetan Plateau

Shuhua Yi[1,2], Yujie He[3*], Xinlei Guo[4], Jianjun Chen[5,6], Qingbai Wu[7], Yu ~~Qin[1]~~ Qin[2], and Yongjian ~~Ding[1]~~Ding[2,8,9]

~~[1.] State Key Laboratory of Cryospheric Sciences, Northwest Institute of Eco-Environment and Resources, Chinese Academy of Sciences, 320 Donggang West Road, 730000, Lanzhou, Gansu, China~~

[~~2~~1.] School of Geographic Sciences, Nantong University, 999 Tongjing Road, Nantong, 226007, China

[2.] State Key Laboratory of Cryospheric Sciences, Northwest Institute of Eco-Environment and Resources, Chinese Academy of Sciences, 320 Donggang West Road, 730000, Lanzhou, Gansu, China

[3.] Chinese Research Academy of Environmental Sciences, No.8 Dayangfang, Chaoyang District, 100012, Beijing, China

[4.] Department of Ecosystem and Landscape Dynamics, Institute for Biodiversity and Ecosystem Dynamics, University of Amsterdam, Science Park 904, 1098 XH Amsterdam, The Netherlands~~Forschungszentrum Jülich GmbH, Institute of Bio- and Geosciences, Agrosphere (IBG-3), Wilhelm-Johnen-Straße, 52428 Juelich, Germany~~

[5.] College of Geomatics and Geoinformation, Guilin University of Technology, 12 Jiangan Road, Guilin, 541004, China

[6.] Guangxi Key Laboratory of Spatial Information and Geomatics, 12 Jiangan Road, Guilin, 541004, China

[7.] State Key Laboratory of Frozen Soil Engineering, Northwest Institute of Eco-Environment and Resources, Chinese Academy of Sciences, 320 Donggang West Road, 730000, Lanzhou, Gansu, China

[8.] Key Laboratory of Ecohydrology of Inland River Basin, Chinese Academy of Sciences, Lanzhou 730000, China

[9.] University of Chinese Academy Sciences, Beijing, 100049, China

*Co-first Author

Correspondence to: Yongjian Ding (dyj@lzb.ac.cn)

Abstract. Soils on the Qinghai-Tibetan Plateau (QTP) have distinct physical properties from agricultural soils due to weak weathering and strong erosion. These properties might affect permafrost dynamics. However, few studies have investigated both quantitatively. In this study, we selected a permafrost site on the central region of the QTP and excavated soil samples down, to 200 cm. We measured soil porosity, thermal conductivity, saturated hydraulic conductivity and matric potential in the laboratory. Finally, we ran a simulation model replacing default sand or loam parameters with different combinations of these

measured parameters. ~~Results~~ Our results from the soil profile showed that coarse soil fragment content (diameter >2 mm) was ~55% on average in soil profile~~;~~, soil porosity was less than 0.3 m^3 m^{-3}~~;~~, saturated hydraulic conductivity ranged from 0.004-0.03 mm s^{-1}~~;~~, saturated matric potential ranged from -14 to -604 mm. When default sand or loam parameters were substituted with these measured values, the model errors of soil temperature, soil liquid water content, active layer depth and permafrost lower boundary were reduced. The root mean squared errors of active layer depths simulated using measured parameters~~, and~~ versus the default sand and loam parameters were about 0.28, 1.06, 1.83 m, respectively. Among these measured parameters, porosities, which were much smaller than for soil textures used in land surface models, played a dominant role in reducing model errors. We also demonstrated that soil water dynamic processes should be considered, rather than using static properties under frozen and unfrozen soil states as in most permafrost models. We conclud~~eed~~e that it is necessary to consider the distinct physical properties of soil and water dynamics on the QTP when simulating dynamics of permafrost. It is important to develop methods for systematic measuring physical properties of coarse soil fragment and to develop a spatial dataset for porosity because of its importance in simulating permafrost dynamics in this region.

Key words: Terrestrial Ecosystem Model; Active ~~L~~layer; Sensitivity ~~Test~~test; Soil ~~Temperature~~temperature; Soil ~~Water~~ water ~~Content~~content; Porosity; Coarse ~~soil~~ fragment soils

1 Introduction

Permafrost covers 25% of ~~the earth~~Earth's surface. Degradation of permafrost has been reported extensively in Alaska, Siberia and the Qinghai-Tibetan Plateau (QTP; Boike et al., 2013; Jorgenson et al., 2006; Wu and Zhang, 2010). ~~It~~ Permafrost thaw has global impacts by releasing large quantities of soil carbon previously preserved in a frozen state and enhancing concentrations of atmospheric greenhouse gases, which will promote further atmospheric warming and degradation of permafrost (Anisimov, 2007; McGuire et al., 2009). Permafrost dynamics also have local to regional impacts on ecosystems by altering soil thermal and hydrological regimes (Salmon et al., 2015; Wang et al., 2008; Wright et al., 2009; Ye et al., 2009; Yi et al., 2014a). In addition, degradation of permafrost affects infrastructure, ~~e.g.~~such as QTP railways and roads (Wu et al., 2004)~~, and~~ or the Trans-Alaska Pipeline System in

带格式的：上标

带格式的：上标

Alaska (Nelson et al., 2001). Therefore, it is critical to develop mitigation and adaptation strategies in permafrost regions for ongoing climate change. Accurate projection of the degree of permafrost degradation is a prerequisite for developing these strategies.

Significant effort has been made to improve modeling accuracy and efficiency of permafrost dynamics along two primary lines of inquiry. One is to create suitable freezing and thawing algorithms for different applications, including land surface models (Chen et al., 2015; Oleson et al., 2010; Wang et al., 2017), permafrost models (Goodrich, 1978; Langer et al., 2013; Qin et al., 2017), and other related models (Fox, 1992; Woo et al., 2004). The other line of inquiry is focused on schemes of soil physical properties (Chen et al., 2012; Zhang et al., 2011), which play a critical role in permafrost dynamics. For example, ~~thermal diffusivity (thermal conductivity/heat capacity) directly determines how quickly energy can be conducted into and out of permafrost from the top and from the bottom of the permafrost horizon. Porosity~~ porosity determines the maximum amount of water that can be contained in a soil layer, thermal properties determine the heat conduction within soil layers, and hydraulic properties determine the exchange of soil water between soil layers. The ~~amount of water then affects not only soil thermal properties, but~~soil water content also determines the large amount of latent heat ~~loss/gain~~lost or gained ~~for freezing/thawing~~by freezing or thawing, respectively. On the QTP, soil is coarse due to weak weathering and strong erosion (Arocena et al., 2012). Soils with gravel content (particle diameter >2 mm) ~~has~~ have been reported in several studies (Wang et al., 2011; Wu et al., 2016; Yang et al., 2009; Qin et al., 2015; Chen et al., 2017; Du et al., 2017). These gravelly soil properties are likely different from those used in current modeling studies (Wang et al., 2013). For example, ~~Soil~~ soil properties in Community Land Model are calculated from fractions of sand, silt and clay based on measurements of agriculture soils (Oleson et al., 2010). However, ~~those~~ soil properties of ~~gravelly~~ coarse fragment soil on the QTP and their effects on permafrost dynamics are under studied (Pan et al., 2017).

In this case study we investigated the characteristics of soil physical properties at a site on the central QTP and ~~its~~ their effects on permafrost dynamics. We first measured soil physical properties of excavated soil samples in a laboratory. We then conducted sensitivity ~~analyses~~ analysis with an ecosystem model by substituting the default soil physical properties ~~by~~ with those that we measured. We aimed to emphasize the effects of ~~gravel~~ coarse fragment content on soil physical properties and on permafrost dynamics~~. It is not our purpose~~ , rather than ~~to~~ develop general schemes of soil physical properties for using in modeling studies on the QTP.

2 Methods

2.1 Site description

The site (34°49’46.2” N, 92°55’56.58” E, 4,628ma.s.l.) is located in the Beiluhe basin~~. This basin is~~, in the continuous permafrost region of the central QTP (Figure 1a, Zou et al. 2017). Based on the ~~soil~~ map of Li et al. (2015), soils of this region belong~~s~~ to Gelisols and Inceptisols, which occupy 34% and 28% of the total area of permafrost region of the QTP, respectively. Land surface types include alpine meadow, alpine steppe, barren surface and thermokarst lakes (Figure 1b; Lin et al., 2011).

The site is on top of upland plain landforms, which are formed ~~with~~ from fluvial and deluvial sediments. The surficial sediments are dominated by fine to gravelly sands and stones (Figure 2; Yin et al., 2017). Soil of this site belongs to Inceptisols (Dr. Li, Wangping of Lanzhou University of Technology, personal communication). Mudstone is common beneath soil. The plant community type is mainly alpine meadow which is dominated by monocotyledonous species, primarily Poaceae and Cyperaceae. The dominant species are *Kobresia pygmaea*, accompanyed *Elymus nutans*, *Carex moorcroftii*, *Oxytropis pusilla*, *Tibetia himalaica*, *Leontopodium nanum* and *Androsace tapete* (Figure 2c-e).

A weather station was set up in 2002 (Figure 2a~~).~~) to measure ~~Air~~ air temperature and relative humidity (2.2m, HMP45C-L11 /L36, Campbell Scientific Inc.), solar radiation (MS-102, EKO, Japan) and~~,~~ precipitation (QMR102, Vaisala Company)~~ were measured~~. Soil temperatures were measured at depths of 5, 10, 20, 40, 80 and 160 cm using a PT-100 (EKO, Japan); soil moistures were measured at depths of 20, 40, 80 and 160 cm using a CS616-L50 (EKO, Japan). A CR3000 data logger (Campbell Scientific Inc., USA) was used to store these data at ~~an interval of~~ 30 ~~minutes~~minute intervals. These ~~halfhour values~~readings were averaged or summed (e.g. precipitation) into monthly values ~~for model driving and validation~~to drive and validate the model. Based on measurements, multi-year mean annual air temperature, precipitation, downward solar radiation and relative humidity were -3.61 °C, 365.7 mm, 206.3 W ~~/m^2~~ m^{-2} and 51.1%, respectively (Figure 3). The multi-year mean summer (June to August)~~/winter (December to February)~~ air temperature and precipitation were 5.27~~/-12.44~~ °C and 248.3~~/5.3~~ mm, respectively. The multi-year mean winter (December to February) air temperature and precipitation were -12.44 °C and 5.3 mm, respectively. The multi-year mean annual, summer, winter soil temperature at 40~~/80~~ cm were 0.17~~/0.11~~, 6.65~~/4.32~~ and -7.15~~/-4.86~~ °C, respectively. Those at 80 cm were 0.11, 4.32 and -4.86 °C, respectively

A borehole was drilled in 2002~~.~~, and ~~Temperature~~ thermistors made by the State Key Laboratory of Frozen Soil Engineering, Chinese Academy of Sciences were installed at 0.5 m intervals from 0.5 to 10 m, at 2 m intervals from 12 to 30 m, at 4 m intervals from 34 to 50 m, ~~at depths between 0.5 m and 10 m with interval of 0.5 m; at depths between 12 m and 30 m with interval of 2 m; at depths between 34 m and 50 m with interval of 4 m;~~ , and at 55 and 60 m. Temperature accuracy of this type of thermistor is ±0.05 °C (Wu et al., 2016). The temperatures were recorded on the 5th and 20th days of each month using CR3000 data logger (Campbell Scientific Inc., USA). Based on measurement, active layer depth is ~3.3 m~~.~~, depth of zero annual amplitude is ~6.2 m, and the lower boundary of permafrost is at a depth of ~20 m. The multi-year mean ground temperatures at 0.5, ~~12~~6, and 60 m are about -0.52, -0.~~29~~ 30 and 1.81 °C, respectively.

2.2 Soil sampling and measurement

Permafrost dynamics are affected by atmosphere, vegetation, and soil textures, therefore, we excavated soil close to the weather station and borehole (Figure 2a) down to 2 m (Figure 2b) in August 2014. We used cut rings (10 cm diameter, 6.37 cm height and 500 cm^3) to take soil samples at depth ranges of 0-10, 10-20, 20-30, 40-50, 70-80, 110-120, 150-160, and 190-200 cm. Three replicates were sampled from the top of each depth range and sealed for analysis in the laboratory. Above 120 cm in the soil pit, coarse soil material was small enough ~~to be fitted~~ in the cut rings. Below 150 cm, ~~there exists~~the material is weathered mudstone, which could also be sampled with our cut rings. Based on the excavated soil pit and measured soil temperature, this site belongs to Inceptisols with suborder of Gelept (soil taxonomy, ST, Soil Survey Staff, 2014). The soil pit consists of A horizon (~20 cm), Bw horizon (~20-80 cm) and C material dominated by fractured bedrock.

We used the KD2 Pro (Decagon, US) to measure thermal conductivity of soil samples. The steps we took to determine soil properties for each sample were as follows ~~were~~: 1) soil sample~~s~~ ~~were~~ was dried in an oven and weighed (0.001g precision) to calculate bulk density; Then 2) the soil sample~~s~~ ~~were~~ was exposed to a constant temperature (20°C) ~~over~~ for 24 h, a certain volume of water was injected into the soil samples, and ~~the~~ KD2 Pro (Decagon, USA) was used to measure the thermal conductivity ~~of the soil samples~~. , Next 3) the sample~~s~~ and the KD2 probe were ~~then~~ put into a refrigerator ~~(0~-26°C)~~ at -15°C ~~over~~ for 12 h~~,~~ and thermal conductivity was ~~then~~ measured again; 4) Steps 2 and 3 were repeated at ~~different~~ increasing levels of soil volumetric water content until soil samples were ~~about to be saturated~~up to the point of saturation. Finally 5) ~~Finally~~, the soil sample~~s~~ ~~were~~ was immersed in~~to~~ water ~~over~~ for 24 h and weighed to calculate porosity~~; ~~, and the saturated unfrozen and frozen thermal conductivity were then measured, accordingly. The bulk density (BD), porosity (PORO) and volumetric water content (VWC) were calculated with the following equations.

$$BD = \frac{W_{dry} - W_{cr}}{V_{cr}} \quad (1)$$

$$PORO = \frac{W_{sat} - W_{dry}}{V_{cr}} / \rho \quad (2)$$

$$VWC = \frac{W_{all} - W_{dry}}{V_{cr}} / \rho \quad (3)$$

Where W_{dry}, W_{sat}, W_{all}, W_{cr} are ~~weight~~ mass of over dried sample, saturated sample, sample with some water with cut ring, and empty cut ring (g), respectively. V_{cr} is the volume of cut ring (cm^3). ρ is the density of water (1 g~~/~~ cm^{-3}). We used pressure membrane instruments (1500F1, Soilmoisture Equipment Corp, US) to measure the matric potential of soil samples (Azam et al., 2014; Wang et al., 2007)~~. In this study we used~~, using both 15 bar and 5 bar pressure chambers. Pressure values were set at 0, 10, 20, 40, 60, 80, 100, 150, 200, 300, and 400 kpa. It usually took 3-4 days to finish one measurement at one pressure level. We used a soil permeability meter (TST-70, Nanjing T-Bota Scietech Instruments & Equipment Co., Ltd. China) to measure saturated hydraulic conductivity of soil samples (Gwenzi et al., 2011). Finally, soil samples were sieved through a 2.0 mm mesh ~~meshes with diameters of 2.0 mm~~, and soil particle size distribution was determined with a ~~Malvern~~ laser diffraction analyzer (Malvern-2000, ~~Instruments Inc.~~ Worcestershire, UK).

2.3 Model description

The model used in this study is a dynamic organic soil version of Terrestrial Ecosystem Model (DOS-TEM). Models ~~of~~ from the TEM family simulate the carbon and nitrogen pools of vegetation and soil, and their fluxes among atmosphere, vegetation, and soil (McGuire et al., 1992). They have been widely used in studies of cold region ecosystems (e.g. McGuire et al., 2000; Yuan et al., 2012; Zhuang et al., 2004; 2010). The DOS-TEM consists of four modules, ~~these being the~~ environmental, ecological, fire disturbance, and dynamic organic soil ~~modules~~ (Yi et al., 2010). The environmental module operates on a daily time interval

带格式的: 下标

带格式的: 上标

using mean daily air temperature, surface solar radiation, precipitation, and vapor pressure, which are downscaled from monthly input data (Yi et al., 2009b). The module takes into account radiation and water fluxes among the atmosphere, canopy, snow pack, and soil. Soil temperatures, soil liquid water content, temperature in rock layers, active layer depth (ALD) and permafrost low boundary (PLB) were simulated explicitly.

2.3.1 Implementation of soil thermal processes

Earlier versions of TEM did not simulate soil temperature (McGuire et al., 1992). Zhuang et al. (2001) incorporated Goodrich (1978) permafrost model into TEM. Yi et al. (2009a) incorporated a two-directional Stefan algorithm to simulate soil freezing and thawing for complex soils ~~situation~~ with changes ~~of organic soil~~in soil organic and moisture content. ~~Soil t~~Temperatures of all soil layers in the DOS-TEM are updated daily. Phase change is calculated first before heat conduction. A two-directional Stefan algorithm is used to predict the depths of freezing or thawing fronts within the soil (Woo et al., 2004). It first simulates the depth of the front in the soil column from the top downward, using soil surface temperature as the driving temperature. It then simulates the front from the bottom upward using the soil temperature at a specified depth beneath a front as the driving temperature (bottom-up forcing). The latent heat used for phase change is recorded for each soil layer. If a layer contains *n* freezing or thawing fronts, this layer is then explicitly divided into *n*+1 soil layers. All soil layers are grouped into 3 parts: 1) ~~the soil layers~~ those above the uppermost freezing or thawing front; 2) ~~the soil layers~~those below the lowermost freezing or thawing front; and 3) ~~the soil layers~~those between the uppermost and lowermost fronts. Soil temperatures are then updated by solving finite difference equations of each part with latent heat from phase change ~~latent heat~~ as an energy source or sink (Yi et al., 2014a). Soil surface temperature, which is used as a boundary condition, is calculated using daily air maximum, air minimum, radiation, and leaf area index (Yi et al., 2013).

The version of the DOS-TEM in this study uses the Côté and ~~Konard~~Konrad (2005) scheme to calculate thermal conductivity (Yi et al., 2013; Pan et al., 2017), which is also been used by other studies on the QTP (e.g. Chen et al., 2012, Luo et al., 2009), and is as follows:~~.~~

$$\lambda = \begin{cases} k_e\lambda_{sat} + (1 - k_e)\lambda_{dry} & s > 10^{-5} \\ \lambda_{dry} & s \le 10^{-5} \end{cases} \quad (4)$$

where λ, λ_{sat}, λ_{dry} are soil thermal conductivity, saturated soil thermal conductivity, and dry soil thermal conductivity (W m^{-1} K^{-1}), respectively, and. k_e is the Kersten number (Côté and Konrad, 2005). Dry thermal conductivity varies with soil properties according to:

$$\lambda_{dry} = \chi 10^{-\eta\phi} \quad (5)$$

where χ (W m^{-1} K^{-1}) and η (no unit) are parameters accounting for particle shape effects, which are specified for gravel, fine mineral and organic soil (Côté and KonardKonrad, 2005).), and ϕ is porosity. Saturated thermal conductivity varies with water content and phase state according to:

$$\lambda_{sat} = \begin{cases} \lambda_s^{1-\phi}\lambda_{liq}^{\phi} & T \le T_f \\ \lambda_s^{1-\phi}\lambda_{ice}^{\phi} & T > T_f \end{cases} \quad (6)$$

where λ_{liq}, λ_{ice}, λ_s are thermal conductivitiesy of liquid water, ice, and soil solid (W m^{-1} K^{-1}), which are all constant values. T and T_f are temperature of soil and freezing point temperature of soil (°C), respectively. In DOS-TEM, freezing or thawing processes are assumed to be happened at T_f, following most of the land surface models (e.g. Oleson et al. 2010).

带格式的：下标

2.3.2 Implementation of soil hydrological processes

Surface runoff, infiltration, and water redistribution among soil layers are simulated in a similar way as Community Land Model 4 (Oleson et al., 2010). Soil matric potential (Ψ) determines the direction of water movement. A, and hydraulic conductivity describes the ease with which water can move through the soil pore.

$$\Psi = \Psi_{sat}(\frac{\theta_{liq}}{\phi})^{-B} \quad (7)$$

where Ψ_{sat} is saturated soil matric potential (mm H_2O, hereafter mm), θ_{liq} is volumetric liquid water content (m^3 m^{-3}), and B is pore size distribution parameter. The soil hydraulic conductivity (K, mm s^{-1}) is a function of the saturated soil hydraulic conductivity (K_{sat}) as follows:

带格式的：上标

带格式的：下标

$$K = K_{sat}(\frac{\theta_{liq}}{\phi})^{2B+3} \quad (8)$$

where K is soil hydraulic conductivity, and K_{sat} is saturated soil hydraulic conductivity (mm s^{-1}).

Several important features relating to permafrost have been considered in the DOS-TEM (see Yi et al., 2014b), ~~e.g.~~including runoff from a perched saturated zone ~~and~~ or exchanges of water between the soil and a water reservoir. Runoff from ~~the~~ a perched saturated zone above ~~the~~ permafrost is implemented following Swenson et al. (2013):~~,~~

$$Q_{perch} = \alpha k_p (z_{frost} - z_{perched}) \sin(\frac{\Theta}{180}\pi) \quad (9)$$

~~Where~~ where α is an adjustable parameter (0.6 m^{-1}), K_p is the mean saturated hydraulic conductivity within the perched saturated zone (mm s^{-1}), z_{frost} and $z_{perched}$ are the depths to the permafrost table and the perched water table (m), respectively, and Θ ~~θ~~ is slope (°).

The DOS-TEM has been verified against the Neumann Equation for water, mineral and organic soil under an idealized condition (Yi et al., 2014b), and validated against field measurements for various locations in Alaska, the Arctic, and the QTP (Yi et al., 2009b, Yi et al., 2013, Yi et al., 2014a).

2.4 Model inputs and initialization

We used the ~~measured~~ monthly averaged air temperature, downward radiation, precipitation and humidity ~~(monthly)~~ as input to drive the DOS-TEM. Leaf area index (LAI), ~~one-sided green~~ leaf area per unit ground surface area, was specified to be 0.6 m^2m^{-2} in July and August, 0.1 m^2m^{-2} in April and October, 0 m^2m^{-2} between November and March, and interpolated linearly in other months. It is used in the DOS-TEM to calculate ground surface temperature in combination with other meteorological variables (Yi et al., 2013). Its value is unchanged within each month.

Soil temperature and moisture were initialized at -1 °C and saturation.~~.~~ The temperature gradient at the bottom of bedrock was set to be 0.06 °C cm^{-1} based on borehole observations. Volumetric unfrozen liquid water in winter was set to be 0.1 based on observations. Multi-year (2003-2012) mean ~~(2003-2012)~~ monthly driving data were used ~~for spun~~to spin up the model for 100 yr. In this way, ~~proper~~ suitable initial values of soil moisture, temperature and rock temperature of each layer ~~can be~~are generated ~~for the beginning of 2003. Finally, monthly driving data were used to drive DOS-TEM~~ before driving DOS-TEM with monthly data over the period of 2003-2012.

2.5 Sensitivity analyses

The soil textures on the QTP mainly consist of loam, sand, and ~~gravel~~ coarse soil fragments (Wu and Nan, 2016). We used a uniform sand ~~and~~ or loam ~~in whole~~ soil profile ~~uniformly~~ to represent coarse and fine soil textures, respectively. ~~The parameters of coarse soil textures are not~~Sands are the most coarsest texture considered in most ~~of~~ the modeling studies (e.g. Oleson et al., 2010). Therefore, we used our measured parameters to substitute the parameters of sand and loam to investigate the effects of coare-fragment soil parameters on permafrost dynamics. We first ran ~~the~~ DOS-TEM using the default porosity, soil thermal conductivity (Equation 4), hydraulic conductivity (Equation 8), and matric potential schemes of these two default soil textures (Equation 7). The default parameters Φ, Ψ_{sat}, K_{sat} and B were calculated based on soil texture used in Community Land Model (Equation 7 and 8; Oleson et al., 2010). We then substituted the default values of Φ, Ψ_{sat}, K_{sat} and B based on our laboratory measurements and calibration. ~~Saturated matric potential~~Parameters Ψ_{sat} and B were fitted with measured matric potential data using Isqucurvefit tools of Matlab. We did not calibrate soil thermal conductivity to retrieve parameters of Equation 5 and 6. Instead, we interpolated measured thermal ~~conductivity~~ conductivities over a range of ~~the~~ degrees of saturation (0 to 1), which was used as a lookup table by the DOS-TEM. Therefore, our sensitivity analyses considered a set of 4 factors, i.e. porosity, matric potential (Ψ_{sat} and B), hydraulic conductivity (K_{sat} and B) and thermal conductivity. We also analyzed 3 different slopes (0, 5 and 10^{o}) and 3 different soil thicknesses (3.25, 4.25 and 5.25 m) above 56 m of bed rock. There ~~are~~ were 11 soil layers with the top 9 layers being 0.05, 0.1, 0.1, 0.2, 0.2, 0.2, 0.3, 0.3 and 0.3 m thick. The thicknesses of the bottom 2 soil layers ~~are~~ were 0.5 and 1 m, 0.5 and 2 m, and 1.5 and 2 m for the 3.25, 4.25 and 5.25 m cases, respectively. There ~~are~~ were 6 rock layers with thicknesses of 2, 2, 4, 8, 16 and 20 m. Since the site is on the top of upland plain landforms, we did not further test the effects of aspect on radiation on ground surface. We instead considered the effects of slope on surface runoff. In summary, our sensitivity analyses with the DOS-TEM involved 288 different combinations of parameter values.

We did not measure the heat capacity. The maximum and minimum heat capacities of mineral soil types considered in land surface model are 2.355 and 2.136 MJ m^{-3}, respectively~~. The~~ , giving a relative difference ~~is~~ less than 10%. Therefore, in this study, we did not make sensitivity tests using thermal diffusivity (the ratio between thermal conductivity and heat capacity).

3 Results

3.1 Soil physical properties

3.1.1 Soil porosity, particle size and bulk density

Results from laboratory analysis of the soil samples are shown in Table 1 and 2. The mean weight ~~fraction of gravel~~of the coarse soil fraction (particle size diameter > 2 mm) of different soil layers ranged from 0.38 to 0.65 with a mean of 0.55~~ (Table 1)~~. According to the USDA classification system (clay (<2 μm), silt (2 –50 μm, in this study 2-63 μm) and sand (50 μm -2.0 mm, in this study 63 μm -2.0 mm)), the major soil texture of this site was loamy sand, with the exception of sandy loam at depth of 20-30 cm~~ (Table 1)~~. The default porosities of sand and loam were 37.3% and 43.5%, respectively. The measured~~mean~~ porosity of samples ~~in~~ down to 2 m depth ranged from 21% to 30% with a mean of 27%~~. The~~, and the mean bulk density ranged from 1.61 to 1.86 g cm^{-3} with a mean of 1.74 g cm^{-3}. The porosity calculated from bulk density (= 1- bulk density/2.65 g cm^{-3}) ranged from 29.8% to 39.2%. No significant relationships were found among soil porosity, bulk density and the ~~fraction of gravel~~coarse soil fraction ($p>0.05$).

3.1.2 Thermal conductivity

The results of the thermal conductivity determinations are shown in Table 3. The ~~mean~~ unfrozen dry soil thermal conductivity of different soil layers ranged from 0.24 to 0.40 W m^{-1} K^{-1} with a mean of 0.36 W m^{-1} K^{-1} ~~(Table 2).~~, and ~~The~~ the~~mean~~ frozen dry soil thermal conductivity ranged from 0.25 to 0.41 W m^{-1} K^{-1} with a mean of 0.35 W m^{-1} K^{-1}. The difference of dry thermal conductivity between frozen and unfrozen states was small. The ~~mean~~ unfrozen saturated soil thermal conductivity of different soil layers ranged from 2.15 to 2.74 W m^{-1} K^{-1} with a mean of 2.48 W m^{-1} K^{-1}~~ (Table 2)~~. The~~ mean~~ frozen saturated soil thermal conductivity ranged from 3.06 to 3.72 W m^{-1} K^{-1} with a mean of 3.33 W m^{-1} K^{-1}. The difference of saturated thermal conductivity between frozen and unfrozen states was about 0.85 W m^{-1} K^{-1}. There existed a threshold of soil wetness (i.e. ~0.28 m^{3} m^{-3}), below which frozen soil thermal conductivity was slightly smaller than unfrozen soil (Figure 4a).

Results from determining thermal conductivities using the Côté and Konrad (2005) scheme are shown in Figure 4b. The default dry frozen and unfrozen thermal conductivities ~~using~~

带格式的: 上标

带格式的: 上标

~~Côté and Konard (2005) scheme of~~for sand and loam were about 0.42 and 0.24 W m^{-1} K^{-1}, respectively. The saturated frozen and unfrozen thermal conductivities of sand were 3.11 and 1.90 W m^{-1} K^{-1}, respectively. Those of loam were about 2.36 and 1.33 W m^{-1} K^{-1}, respectively ~~(Figure 4b)~~. Results from determining thermal conductivities using the Farouki (1986) scheme are shown in Figure 4c. The default dry frozen and unfrozen thermal conductivities ~~using Farouki scheme of~~for sand and loam were about 0.97 and 0.63 W m^{-1} K^{-1}, respectively. The saturated frozen and unfrozen thermal conductivities of sand were 5.21 and 3.18 W m^{-1} K^{-1}, respectively. Those of loam were about 4.49 and 2.52 W m^{-1} K^{-1}, respectively~~ (Figure 4c)~~.

3.1.3 Saturated hydraulic conductivity

The mean saturated hydraulic conductivity of soil layers, shown in Table 4, ranged from 0.0036 to 0.0315 mm s^{-1}. The maximum saturated hydraulic conductivity was about 8.7 times larger than the minimum~~ (Table 3)~~. The saturated hydraulic conductivity tended to be larger with increasing proportion of coarse fragment in the soil samples (Figure 5a), and was about 0.03-0.06 mm s^{-1} for some samples with coarse fragment greater than 70%. The default saturated hydraulic conductivities of sand and loam were 0.024 and 0.0042 mm s^{-1}, respectively.

3.1.4 Matric potential

The correlation coefficients between calculated and fitted matric potential, shown in Table 4, were all greater than 0.96. The mean absolute value of saturated matric potential of soil layers ranged from ~~27.02~~14.47 to 603.7 mm, and those of B ranged from 1.89 to 5.22~~ to 1.89~~ (Table ~~3~~ 4 and Figure 5b). The default absolute value of saturated matric potential of sand and loam were 47.29 and 207.34 mm, respectively, and the B values 3.39 and 5.77, respectively.

3.2 Comparisons between simulations using default vs. measured parameters

3.2.1 Soil temperature

The mean root mean squared errors (RMSEs) between monthly measured soil temperatures and model runs with measured parameters using different combination of soil thicknesses (3.25, 4.25 and 5.25 m) and slopes (0, 5 and 10°) were about -1.07 °C at 20 cm (Figure 6c). The mean RMSEs for all model runs with default sand and loam parameters were about 0.97 and 1.18 °C, respectively. For other soil layers, the RMSEs of model runs with measured parameters were much smaller than those with default sand and loam parameters (Figures 6d-l). The simulated soil temperatures using default sand and loam parameters were all lower than measured ones in summer at 100 and 200 cm; and in winter at 400 cm. The RMSEs can be as large as 2.53 ^{o}C (Figure 6e).

The standard deviations of soil temperatures among different slopes and soil thicknesses using measured parameters were larger than those using the default parameters (Figure 6); and they increased from 0.40 ^{o}C at 100 cm to 0.61 ^{o}C at 200 cm (Figure 6f and i). The standard deviations using default loam parameters were smaller (<0.15 ^{o}C at all depths) than those using default sand parameters.

3.2.2 Soil liquid water

The mean RMSEs between monthly measured liquid soil volumetric water content (VWC) and model simulations with measured parameters ranged from 0.03 to 0.09, which were smaller than RMSEs for sand and loam parameters (Figure 7). The model simulations for loam parameters have larger RMSEs than those for sand parameters. VWCs were always overestimated in warm seasons at depths of 10, 40 and 80 cm. VWCs were underestimated at a depth of 160 cm, where the simulated soil was frozen. All model simulations overestimated VWC at 40 cm, where the maximum measured VWCs were about 0.1 (Figure 7d-f).

The standard deviations of VWC among different slopes and soil thicknesses using sand parameters were about 0.077, which were larger than those using measured parameters (~0.062). The standard deviations of VWC using loam parameters (<0.032) were less than those using measured parameters.

3.2.3 Active layer depth (ALD)

The mean RMSEs between measured ALDs (derived from linear interpolation of soil temperatures) and modelled ALDs (simulated explicitly) were about 1.06, 1.72 and 0.28 m for model runs with sand, loam and measured parameters (Figure 8a). The mean standard deviations were about 0.088, 0.026 and 0.28 m. All simulations using sand and loam parameters underestimated ALDs.

3.2.4 Permafrost lower boundary (PLB)

The mean RMSEs between measured PLBs (derived from linear interpolation of temperatures) and modelled PLBs (derived from linear interpolation of simulated bed rock temperatures) were about 10.25, 10.23 and 6.71 m for model runs with sand, loam and measured parameters (Figure 6b). The mean standard deviations were about 1.89, 1.51 and 6.62 m. All simulations using sand and loam parameters overestimated PLBs.

3.3 Model sensitivity analyses

Deep soil layers used in models are usually specified as being thick. For example, a 1 m thick soil layer was used in our simulations starting around 3 m soil depth. Soil temperatures at this depth are usually close to 0^{o}C. Therefore, the RMSEs of deep soil layers were small and did not facilitate evaluation of model sensitivities. In the following subsections, we used 20 and 100 cm soil temperatures, ALDs and PLBs for sensitivity analysis.

3.3.1 Effects of single parameter sensitivity analyses

Porosity

Replacing default sand or loam porosity with measured porosities changed mean RMSEs of soil temperatures (model runs with 3 different slopes and 3 different soil thicknesses at 2 different soil depths) from 1.18 or 1.84 ^{o}C to 1.25 or 1.09 ^{o}C, respectively (Figure 9 and 10). Mean RMSEs of ALD were reduced from 1.06 or 1.72 m to 0.22 or 0.85 m, respectively. Mean RMSEs of PLB were changed from 10.26 or 10.24 m to 6.61 or 10.97 m. Mean RMSEs of VWC were reduced from 0.074 or 0.14 to 0.06 or 0.062 when measured porosities were used for replacing default sand or loam porosity, respectively (Figure 11 and 12).

Thermal conductivity

Replacing default sand or loam thermal conductivity with measured thermal conductivity reduced mean RMSEs of soil temperatures from 1.18 or 1.84^{o}C to 1.02 or 1.15^{o}C, respectively (Figure 9 and 10). Mean RMSEs of ALD were reduced from 1.06 or 1.72 m to 0.56 or 1.04 m, respectively. Mean RMSEs of PLB were changed from 10.26 or 10.24 m to 4.18 or 1.27 m, respectively. Mean RMSEs of VWC changed very slightly (Figure 11 and 12).

Hydraulic conductivity~~/M~~ and matric potential

Replacing default sand or loam hydraulic conductivity with measured parameters had very small effects on mean RMSEs of soil temperatures and ALDs (Figure 9 and 10). The same was true for matric potential. When hydraulic conductivity of default sand or loam was substituted, mean RMSEs of PLB ~~were~~ decreased or increased, respectively. ~~h~~However, when matric potential was substituted, mean RMSEs of PLBs ~~were~~ increased or decreased, respectively. When hydraulic conductivity or matric potential parameters were substituted in default sand or loam parameters, mean RMSEs of VWC changed slightly (Figure 11 and 12).

3.3.2 Effects of combined parameters

We compared model simulations with different combinations of measured parameters (porosity, thermal conductivity, hydraulic conductivity and matric potential) ~~with~~ to those with one substituted measured parameter. We ranked those model runs with less RMSEs than ~~any of~~the best of the model runs with ~~one substituted measured parameter~~ one parameter substituted with a measurement-derived value (Table ~~4~~ 5 and ~~5~~6). We didn’t consider the 10 cm soil temperature, which were similar among all model runs.

For sand, model simulations with porosity and thermal conductivity or hydraulic conductivity substituted had 4 outcomes with lower RMSEs (Table ~~4~~ 5 and Figures 9 and 11). Only 2 out of 7 outcomes had lower RMSEs with all 4 parameters ~~were~~ substituted. Among all the 18 cases with RMSEs less than the individual "best" RMSE, porosity was included 18 times, followed by thermal conductivity and hydraulic conductivity both with 10 times.

For loam, model simulations with porosity and thermal conductivity substituted had 5 outcomes with lower RMSEs (Table ~~5~~ 6 and Figures 10 and 12). Among all the 27 cases with RMSEs less than the individual “best” RMSE, porosity was included 27 times, followed by thermal conductivity with 16 times, and matric potential with 14 times.

3.3.3 Effects of slope and soil thickness

Changes of slope alone had small effects on simulated soil temperatures and ALDs (Figures 9 and 10). An increase of slope generally reduced RMSEs of VWCs (Figures 11 and 12). Model simulations with porosity substituted had smaller differences ~~of~~ in VWC RMSE between different cases of slopes. For example, the mean RMSEs of model simulations with slopes of 0^o or 5^o and ~~porosity substituted in default~~ sand parameters substituted with measured porosity were 0.078 or 0.048, respectively. While those with porosity not substituted were

0.141 or 0.055, respectively. Similarly, the mean RMSEs of model simulations using default loam parameters with porosity substituted were 0.08 or 0.05 for slope of 0^o or 5^o, respectively. The mean RMSEs were 0.18 or 0.1 with porosity not substituted, respectively. For a further increase of slope to 10^o, changes of RMSEs of VWCs at depths of 10-160 cm were small.

Soil thickness had small effects on 20 and 100 cm soil temperatures and 10-160 cm VWCs, and it had prominent effects on PLB for a few cases only with a slope of 10^o (Figures 9 and 10).

4 Discussion

4.1 Characteristics of soil physical properties

Although the effects of coarse fragment soil on permafrost dynamics have been considered in a few modelling studies, the thermal and hydraulic properties of coarse fragment soil were calculated without validation or calibration (Pan et al., 2017; Wu et al., 2018). To our knowledge, this is the first study measuring physical properties of coarse fragment soil samples from permafrost region of the QTP.

The weight fraction of coarse fragment (diameter > 2mm, including gravel) in the soil samples we analysed was greater than 55% on average. While the typical soil types considered in land surface models and other models usually have much smaller diameter. For comparison, the fractions of gravel considered in Pan et al. (2017) ranges from 5% to 33% and from 10% to 28% for the Madoi and Naqu sites, respectively. The Beiluhe site and the aforementioned sites are located in regions with Gelisols and Inceptisols, which occupy ~62% of the permafrost regions of the QTP (Li et al., 2015). It is possible that coarse fragment soil commonly exists on the QTP. The dataset of Wu and Nan (2016) indicated that gravel content widely exists on the middle and western part of the QTP. The saturated hydraulic conductivity and matric potential of soil samples measured in this study were more similar to sand than to loam (see Section 3.1). It is consistent with the study of Wang et al. (2013) that coarse soil material has poor water holding capability.

The measured thermal conductivities of saturated soil samples were relatively close to those estimated by the Côté and ~~Konard~~Konrad (2005) scheme. But they were much less than those estimated by the Farouki scheme (Figure 4). Several other studies also found that Farouki scheme overestimated soil thermal conductivity (Chen et al. 2012; Luo et al., 2009).

One important finding of this study is the relatively small value of porosity. The measured porosity ranged from 0.206 to 0.302, which is less than those of soil types considered in land surface models. For example, the porosities of mineral soil types considered in Community Land Model range from 0.37 to 0.48 (Oleson et al., 2010). Porosity determines the maximum water stored in a soil layer, and affects soil thermal conductivity, hydraulic conductivity and matric potential (Equation 5-8). It plays a more important role than other parameters in simulated soil thermal and hydrological dynamics (Table 4 5 and 56; Figure 9-12). It is noteworthy that it is easy and efficient to measure porosity.

4.2 Effects of soil water on permafrost dynamics

Soil water not only affects soil thermal properties, (e.g. thermal conductivity and heat capacity), but also affects the amount of latent heat lost or gained, for freezing or thawing, respectively (Goodrich, 1978; Farouki, 1986). Soil water is determined by infiltration, evapotranspiration, water movement among soil layers, subsurface runoff and exchange with a water reservoir. Therefore, processes or parameters that affect soil water dynamics will also affect permafrost dynamics. This study quantitatively assessed the effects of soil water on permafrost dynamics. For example, when default loam parameters with high porosity and low saturated hydraulic conductivity were used, soil layers were almost saturated (Figure 7). The simulated ALDs were about 1.58 m, which was less than half of measured ALDs (Figure 8a). When the slope was 0^o, subsurface runoff didn't happen occur in the saturated zone above the bottom of the active layer. The simulated soil water content was generally higher in the active layer. However, when the slope was 5^o, the simulated soil water content was less and the RMSE was smaller (Figure 11 and 12). These patterns were especially obvious when both porosity and saturated hydraulic conductivity were large (Equation 9; Figure 11 and 12). Other studies have also emphasized the importance of subsurface runoff above the bottom of the active layer (Frey and McClelland, 2009; Walvoord and Striegl, 2007). The effects of soil water content on soil thermal dynamics increased with soil and rock depth (Figure 9 and 10). The biggest effects were on PLB, which became manifest during long-term spinup procedures.

Land surface models generally represent soil water dynamics (e.g. Chen et al., 2015; Oleson et al., 2010; Wang et al., 2017). However, the thermal processes in permafrost models usually use specified thermal properties, which were static during model simulations (Li et al., 2009; Nan et al., 2005; Qin et al., 2017; Zou et al., 2017). As shown in this study, soil thermal and hydrological properties depend largely on soil water content. when permafrost degraded, the thermal and hydrological regimes of soil also changed. It is critical to simulate soil water dynamics to properly project permafrost dynamics in the future.

4.3 Limitations and Outlook

4.3.1 Sampling and laboratory measurement

We used cut rings with 10 cm diameter to take soil samples. There aresample soil and weathered mudstones in our study site, which can be sampled in cut rings. However, it is very likely that there are soil samples withcould have been much bigger coarse soil fragment. Therefore, larger containers should be used to take samples for further laboratory analysis in the future.

During our laboratory work, we found two phenomena. First, we originally used the QL-30 thermophysical instrument to measure thermal conductivity. It worked properly under unfrozen condition. However, when frozen, the surface of the soil samples was usually uneven due to frost heave. The, which reduces the contact between the QL-30 plate of QL-30 and the soil sample surface was not ideal. The measured frozen thermal conductivities were smaller than unfrozen thermal conductivity even for the case of saturation, which were definitely wrong., thus we used the KD2 pro to determine thermal conductivities. The second phenomenon was that there seems to be a threshold of soil wetness, below which unfrozen soil thermal conductivity is greater than frozen soil thermal conductivity (Figure 4a). This pattern was somewhat exhibited in estimates of the Côté and KonardKonrad (2005) scheme (Figure 4b), but not in the estimates of the Farouki scheme (Figure 4c). More measurements using instruments with higher accuracy should be made in the future.

It is ideal to draw water in soil samples under a vacuum condition before weighing dry soil sample. Unfortunately, we do not have such instrument. We dried soil samples in an oven at 65 °C for over 48 h, which is commonly used in ecological studies, e.g. Qin et al. (2018). The measured porosities are generally smaller than those calculated from bulk density. We made additional model simulations using porosities calculated from bulk density in combination with other measured parameters. Results showed that the RMSEs of ALD and PLB were 0.55 m and 4.78 m, respectively (Figures not shown). While those used measured porosities were 0.28 m and 6.71 m. Considering the importance of porosity on simulated permafrost dynamics, it is important to draw water out of soil samples in a vacuum condition before weighing dry soil samples in the future.

4.3.2 Model simulation

Although the DOS-TEM using measured parameters provided satisfactory results, there are some aspects requiring further improvement in the future. For example, the measured soil moistures at 40 cm depth were less than 0.1 m^3~~/ m~~^{3}m^{-3}. However, the simulated soil moistures were always much greater (Figure 7f). There were also spikes ~~of~~ in measured soil moistures at 80 and 160 cm depths, which were not presented in the simulation (Figure 7 i and l). In the DOS-TEM, the unfrozen soil water content, or supercold water, was prescribed to be 0.1 m^3/m^3. When soil is freezing, if soil liquid water content is less than this value, no phase change will happen (Figure 7k). ~~It is ideal to~~Therefore, model results would improve with the capability to simulate the dynamics of unfrozen soil water content (Romanovsky and Osterkamp, 2000).

~~Field studies have shown that coarse soil fragment content in root zone affects vegetation growth (Qin et al., 2015), which affects ground surface temperature (Yi et al., 2013). In the current study, we used specified leaf area index. The fractions of coarse fragment content in soil are also dynamic. For example, Chen et al. (2017) found that plateau pika excavated subsurface soil with gravel on to surface. Fine soil particles were carried away by wind and water erosion, which resulted in gravel remaining at the surface. Our ongoing research is working towards representing the coupling of vegetation growth, small mammal disturbances, and soil erosion on permafrost dynamics of the QTP in the future.~~

4.3.3 Regional applications

Soil texture plays an important role in permafrost dynamics (Figure 8). However, the dominant soil texture on the QTP from Wu and Nan (2016) ~~is~~ are loam, sand, and gravel. The specification of loam in simulations results in estimates of ALD that are much smaller than mea~~n~~surements (Yi et al., 2014a). To properly simulate the distribution and dynamics of permafrost on the QTP under climate change scenarios, it is important to develop proper schemes of soil physical properties in relation to coarse fragment content (including gravel) and to develop regional datasets of soil texture for input.

Coarse fragment content affects soil physical properties. For example, soil porosity and saturated hydraulic conductivity are determined by the fraction of gravel, diameter and degree of mixture (Zhang et al., 2011).

Organic soil carbon content in mineral soil on the QTP affects soil porosity and thermal conductivity (Chen et al., 2012). In the site considered in this study, the amount of organic soil carbon in soil was small (Figure 2), and we did not consider the effects of organic soil carbon on soil properties explicitly. Alpine swamp meadow, alpine meadow, alpine steppe and alpine desert are the major vegetation types on the QTP (Wang et al., 2016; see also Figure 1b). Alpine swamp meadow and alpine meadow usually contain fine soil particles and high organic carbon density; while the other two types usually contain coarse soil particle and low organic carbon density (Qin et al., 2015). More laboratory work is needed to develop proper schemes for representing mixed soil with fine mineral, coarse fragment (including gravel) and organic carbon in permafrost models. It is the first priority to develop schemes that make use of porosity data sets, due to its importance and simplicity of measurement.

The development of a spatially explicit dataset of soil texture is also required for regional applications of projecting permafrost changes on the QTP. One way is to collect relevant data through extensive field campaigns (e.g., Li et al., 2015). Currently, gravelly soil has only been mentioned in scientific literature on the QTP (Chen et al., 2015; Wang et al., 2011; Yang et al., 2009). Only recently, a~~n~~ preliminary dataset considering gravel has been created (Wu and Nan, 2016). Ground penetrating radar is a feasible tool to retrieve soil thickness above the coarse soil fragment layer (Han et al., 2016). Aerial photos taken with ~~Unmanned~~ unmanned aerial vehicles ~~has~~ have been used recently ~~(Yi, 2017), and~~to identify coarse soil fragment ~~on the ground surface can be identified easily in aerial photos~~ (Chen et al., 2017; Yi 2017). In combination with ancillary datasets~~,~~ (e.g. geomorphology, topography, vegetation), it is possible to improve the accuracy of spatial datasets of soil texture on the QTP (Li et al., 2015; Wu et al., 2016). Another way is to retrieve soil physical properties using data assimilation technology, ~~e.g.~~such as Yang et al. (2016) who assimilated porosity using a land surface model and microwave data.

带格式的：缩进：首行缩进： 0 字符

5 Conclusions

In this study, we excavated soil samples from a permafrost site on the central QTP and measured soil physical properties in laboratory. Coarse soil fragment content was common in the soil profile and porosity was much smaller than the typical soil types used in land surface models. We then performed sensitivity analysis of these parameters on soil thermal and hydrological processes within a terrestrial ecosystem model. When default sand or loam parameters were substituted with measured soil properties, the model errors of soil temperature, soil liquid water content, active layer depth and permafrost low boundary were generally reduced. Sensitivity analyses showed that porosity played a more important role in reducing model errors than other soil properties examined. Though it is unclear how representative this soil is in the QTP, it is clear that soil physical properties specific to the QTP should be used to properly project permafrost dynamics into the future.

Acknowledgements. We would like to thank Prof. Dave McGuire of University of Alaska Fairbanks for his careful editing; Dr. Yi Sun for vegetation classification; Dr. Xia Cui of Lanzhou University, Mr. Guangyue Liu for determining depth of zero annual amplitude and Mr. Yan Qin for measurements of soil particle size distribution; Prof. Chien-Lu Ping of University of Alaska and Dr. Wangping Li of Lanzhou University of Technology for helping on soil taxonomy; and the editor and two anonymous reviewers for valuable comments. This study was jointly supported through grants provided as part of the National Natural Science Foundation Commission (41422102, 41730751 and 41690142).

References

Anisimov, O. A.: Potential feedback of thawing permafrost to the global climate system through methan emission, Environ. Res. Lett., 2, 045016, doi:10.1088/1748-9326/2/4/045016, 2007. ~~2, 1-7, 2007.~~

Arocena, J., K. Hall, and L.P.: Zhu Soil formation in high elevation and permafrost areas in the Qinghai Plateau (China), Spanish Journal of Soil Sciences, 2, 34-49, 2012.

Azam, G., Grant, C. D., Murray, R. S., Nuberg, I. K.,and Misra, R. K. : Comparison of the penetration of primary and lateral roots of pea and different tree seedlings growing in hard soils. Soil Research, 52, 87-96, 2014.

带格式的: 缩进: 左侧: 0 厘米, 悬挂缩进: 1.77 字符, 首行缩进: -1.77 字符, 段落间距段前: 6 磅

Boike, J., Kattenstroth, B., Abramova, E., Bornemann, N., Chetverova, A., Fedorova, I., and Langer, M.: Baseline characteristics of climate, permafrost and land cover from a new permafrost observatory in the Lena River Delta, Siberia (1998-2011), Biogeosciences (BG), 10, 2105-2128, 2013.
Chen, H., Nan, Z., Zhao, L., Ding, Y., Chen, J., & Pang, Q.: Noah Modelling of the Permafrost Distribution and Characteristics in the West Kunlun Area, Qinghai-Tibet Plateau, China. Permafrost Periglac, 26,160-174, 2015.
Chen, J., Yi, S., and Qin, Y.: The contribution of plateau pika disturbance and erosion on patchy alpine grassland soil on the Qinghai-Tibetan Plateau: Implications for grassland restoration. Geoderma, 297, 1-9, 2017.
Chen, Y., Yang, K., Tang, W., Qin, J., and Zhao, L.: Parameterizing soil organic carbon's impacts on soil porosity and thermal parameters for Eastern Tibet grasslands, Science in China Series D: Earth Sciences (EN), 55, 1001-1011, 2012.
Cote, J. and J. Konrad: A generalized thermal conductivity model for soils and construction materials, Can. Geotech. J., 42, 443-458, 2005.
Du, Z., Y. Cai, Y. Yan, and X. Wang: Embedded rock fragments affect alpine steppe plant growth, soil carbon and nitrogen in the northern Tibetan Plateau, Plant Soil, 420, 79-92, 2017.
Farouki, O. T.:Thermal properties of soils, Cold Reg. Res. and Eng. Lab., Hanover, N. H, 1986.
Fox, J. D.: Incorporating Freeze-Thaw Calculations into a water balance model, Water Resour. Res., 28, 2229-2244, 1992.
Frey, K. E., and McClelland, J. W.: Impacts of permafrost degradation on arctic river biogeochemistry, Hydrol. Process, 23, 169-182, 2009.
Goodrich, E. L.: Efficient Numerical Technique for one-dimensional Thermal Problems with phase change, Int. J. Heat Mass Transfer, 21, 615-621, 1978.
Gwenzi, W., Hinz, C., Holmes, K., Phillips, I. R., and Mullins, I. J.: Field-scale spatial variability of saturated hydraulic conductivity on a recently constructed artificial ecosystem, Geoderma, 166, 43-56, 2011.
Han.X., Liu, J. , Zhang, J., and Zhang, Z.: Identifying soil structure along headwater hillslopes using ground penetrating radar based technique. Journal of Mountain Science, 13, 405-415, 2016.

Jorgenson, M. T., Shur, Y. L., and Pullman, E. R.: Abrupt increase in permafrost degradation in Arctic Alaska, Res. Lett., 33, L02503, doi:10.1029/2005GL024960, 2006.

Langer, M., Westermann, S., Heikenfeld, M., Dorn, W., and Boike, J.: Satellite-based modeling of permafrost temperatures in a tundra lowland landscape, Remote Sensing of Environment, 135, 12-24, 2013.

Li, J., Sheng, Y., Wu, J., Chen, J., and Zhang, X.: Probability distribution of permafrost along a transportation corridor in the northeastern Qinghai province of China. Cold Regions Science and Technology, 59, 12-18, 2009.

Li, W., L. Zhao, X. Wu, Y. Zhao, H. Fang, and W. Shi: Distribution of soils and landform relationships in the permafrost regions of Qinghai-Xizang (Tibetan) Plateau, Chinese Sci. Bull., 23, 2216-2226, 2015.

Lin, Z., F. Niu, H. Liu, and J. Lu: Hydrothermal processes of alpine tundra lakes, Beiluhe Basin, Qinghai-Tibet Plateau, Cold Reg. Sci. Techol., 65, 446-455, 2011.

Luo, S., Lv, S., Zhang, Y., Hu, Z., Ma, Y., Li, S., and Shang, L.: Soil thermal conductivity parameterization establishment and application in numerical model of central Tibetan Plateau, Chinese Journal of Geophysics, 52, 919-928, 2009. (in Chinese with English Abstract)

McGuire, A. D., J. Melillo, E. G. Jobbagy, D. Kicklighter, A. L. Grace, B. Moore, and C. J. Vorosmarty: Interactions Between Carbon and Nitrogen Dynamics in Estimating Net Primary Productivity for Potential Vegetation in North America, Global Biogeochem. Cy., 6(2), 101-124, 1992.

McGuire, A. D., J. S. Clein, J. Melillo, D. Kicklighter, R. A. Meier, C. J. Vorosmarty, and M. C. Serreze: Modelling carbon responses of tundra ecosystems to historical and projected climate: sensitivity of pan-Arctic carbon storage to temporal and spatial variation in climate, Global Change Biol., 6 (Suppl. 1), 141-159, 2000.

McGuire, A. D., Anderson, L. G., Christensen, T. R., Dallimore, S., Guo, L., Hayes, D. J., . and Roulet, N.: Sensitivity of the carbon cycle in the Arctic to climate change. Ecological Monographs, 79, 523-555, 2009.

Nan, Z., Li, S., and Cheng, G.: Prediction of permafrost distribution on the Qinghai-Tibet Plateau in the next 50 and 100 years. Science in China Series D: Earth Sciences, 48, 797-804, 2005.

Nelson, F. E., Anisimov, O. A.,and Shiklomanov, N. I.: Subsidence risk from thawing permafrost, Nature, 410(6831), 889-890, 2001.

Oleson, K. W., Lawrence, D. M., Bonan, G. B., Flanner, M. G., Kluzek, E., Lawrence, P. J., Levis, S., Swenson, S. C., and Thornton, P.: Technical description of version 4.0 of the Community Land Model (CLM), University Corporation for Atmospheric Research, NCAR 2153-2400, 2010.

Pan, Y., S. Lv, S. Li, Y. Gao, X. Meng, Y. Ao, and S. Wang: Simulating the role of gravel in freeze–thaw processon the Qinghai–Tibet Plateau, Theor. Appl. Climatol., 127, 1011-1022, 2017.

Qin, Y., J. E. Hiller, G. Jiang, and T. Bao: Sensitivity of thermal parameters affecting cold-region ground-temperature predictions, Environ. Earth Sci., 68, 1757-1772, 2013.

Qin, Y., Yi, S., Chen, J., Ren, S., and Ding, Y.: Effects of gravel on soil and vegetation properties of alpine grassland on the Qinghai-Tibetan plateau. Ecological Engineering, 74, 351-355, 2015.

Qin Y., Wu, T. , Zhao, L., Wu, X., Li, R., Xie, C., Pang, Q., Hu, G., Qiao, Y., Zhao, G., Liu, G., Zhu, X., and Hao, J.: Numerical Modeling of the Active Layer Thickness and Permafrost Thermal State Across Qinghai-Tibetan Plateau, Journal of Geophysical Research: Atmospheres, doi:10.1002/2017JD026858, 2017.

Qin, Y., Yi, S., Chen, J., Ren, S., and Ding, Y.: Effects of gravel on soil and vegetation properties of alpine grassland on the Qinghai-Tibetan plateau. Ecological Engineering, 74, 351-355, 2015.

Qin, Y., S. Yi, Y. Ding, G. Xu, J. Chen, and Z. Wang: Effects of small-scale patchiness of alpine grassland on ecosystem carbon and nitrogen accumulation and estimation in northeastern Qinghai-Tibetan Plateau, Geoderma, 318, 52-63, 2018.

Romanovsky, V. E. and T. E. Osterkamp: Effects of unfrozen water on heat and mass transport processes in the active layer and permafrost, Permafrost Periglac., 11, 219-239, 2000.

Salmon, V. G., Soucy, P., Mauritz, M., Celis, G., Natali, S. M., Mack, M. C., & and Schuur, E. A.: Nitrogen availability increases in a tundra ecosystem during five years of experimental permafrost thaw, Global Change Biol., 22, 1927-1941, 2016.

Soil Survey Staff. Keys to Soil Taxonomy, 12th ed. USDA-Natural Resources Conservation Service, Washington, DC, 2014.

Swenson, S. C., D. M. Lawrence, and H. Lee: Improved simulation of the terrestrial hydrological cycle in permafrost regions by the Community Land Model, Journal of Advances in Modeling Earth Systems, 4, M08002, doi:10.1029/2012MS000165, 2013.

带格式的：两端对齐

Walvoord, M. A., & and Striegl, R. G.: Increased groundwater to stream discharge from permafrost thawing in the Yukon River basin: Potential impacts on lateral export of carbon and nitrogen. Geophys. Res. Lett., 34, L12402, doi:10.1029/2007GL030216, 2007.

Wang, F. X., Kang, Y., Liu, S. P., & and Hou, X. Y.: Effects of soil matric potential on potato growth under drip irrigation in the North China Plain. Agricultural water management, 88, 34-42, 2007.

Wang, G., Li. Y., Wang. Y., and Wu, Q.: Effects of permafrost thawing on vegetation and soil carbon pool losses on the Qinghai-Tibet Plateau, China, Geoderma, 143, 143-152,2008.

Wang, H., B. Xiao, M. Wang, and Ming'an Shao: Modeling the soil water retention curves of soil-gravel mixtures with regression method on the Loess Plateau of China, PLoS ONE, 8, e59475, doi:10.1371/journal.pone.0059475, 2013.

~~Wang, G., Li. Y., Wang. Y., and Wu, Q.: Effects of permafrost thawing on vegetation and soil carbon pool losses on the Qinghai-Tibet Plateau, China, Geoderma, 143, 143-152,2008.~~

Wang, L., Zhou, J., Qi, J., Sun, L., Yang, K., Tian, L., and Koike, T.: Development of a land surface model with coupled snow and frozen soil physics, Water Resources Research, 53, 5085-5103, doi:10.1002/2017WR020451, 2017.

Wang, X., Liu, G., and Liu, S.: Effects of gravel on grassland soil carbon and nitrogen in the arid regions of the Tibetan Plateau. Geoderma, 166, 181-188, 2011.

Wang, Z., Q. Wang, L. Zhao, X. Wu, G. Yue, D. Zou, Z. Nan, G. Liu, Q. Pang, H. Fang, T. Wu, J. Shi, K. Jiao, Y. Zhao, and L. Zhang: Mapping the vegetation distribution of the permafrost zone on the Qinghai-Tibet Plateau, Journal of Mountain Sciences, 13, 1035-1046, 2016.

Woo, M. K., Arain, M. A., Mollinga, M., and Yi, S.: A two-directional freeze and thaw algorithm for hydrologic and land surface modelling. Geophys. Res. Lett., 31, L12501, doi:10.1029/2004GL019475, 2004.

Wright, N., Hayashi, M., & and Quinton, W. L.: Spatial and temporal variations in active layer thawing and their implication on runoff generation in peat-covered permafrost terrain. Water Resour. Res., 45, W05414, doi:10.1029/2008WR006880, 2009.

Wu, Q., Cheng, G., and Ma, W.: Impact of permafrost change on the Qinghai-Tibet Railroad engineering. Science in China Series D: Earth Sciences, 47, 122-130, 2004.

Wu, Q., and Zhang, T.:. Changes in active layer thickness over the Qinghai-Tibetan Plateau from 1995 to 2007. J. Geophys. Res., 115, D09107, doi:10.1029/2009JD012974, 2010.

带格式的：英语(美国)

Wu, Q., Z. Zhang, S. Gao, and W. Ma: Thermal impacts of engineering activities and vegetation layer on permafrost in different alpine ecosystems of the Qinghai-Tibet Plateau, China, The Cryosphere, 10, 1695-1706, 2016.

Wu, X., Zhao, L., Fang, H., Zhao, Y., Smoak, J. M., Pang, Q., and Ding, Y.: Environmental controls on soil organic carbon and nitrogen stocks in the high-altitude arid western Qinghai-Tibetan Plateau permafrost region, J. Geophys. Res., 121, 176-187, 2016.

Wu, X. and Nan, Z.: A Multilayer Soil Texture Dataset for Permafrost Modeling over Qinghai– Tibetan Plateau, IGARSS, 4917-4920, 2016

Wu, X., Z. Nan, S. Zhao, L. Zhao, and G. Cheng: Spatial modeling of permafrost distribution and properties on the Qinghai-Tibetan Plateau, Permafrost Periglac., DOI: 10.1002/ppp.1971, 2018

Wu, X. and Nan, Z.: A Multilayer Soil Texture Dataset for Permafrost Modeling over Qinghai– Tibetan Plateau, IGARSS, 4917-4920, 2016

Yang, J., Mi, R., & and Liu, J.:Variations in soil properties and their effect on subsurface biomass distribution in four alpine meadows of the hinterland of the Tibetan Plateau of China, Environ. Geol., 57, 1881-1891, 2009.

Yang, K., Zhu, L., Chen, Y., Zhao, L., Qin, J., Lu, H., ., and Fang, N.: Land surface model calibration through microwave data assimilation for improving soil moisture simulations,Journal of Hydrology, 533, 266-276, 2016.

Ye, B., Yang, D., Zhang, Z., and Kane, D. L.: Variation of hydrological regime with permafrost coverage over Lena Basin in Siberia. J. Geophys. Res., 114, D07102, doi:10.1029/2008JD010537, 2009.

Yi S, FragMAP: a tool for long-term and cooperative monitoring and analysis of small-scale habitat fragmentation using an unmanned aerial vehicle, International Journal of Remote Sensing, 38:2686-2697, 2017.

Yi, S., Manies, K. L., Harden, J., and McGuire, A. D.: The characteristics of organic soil in black spruce forests: Implications for the application of land surface and ecosystem models in cold regions, Geophys. Res. Lett., 36, L05501, doi:10.1029/2008GL037014, 2009a.

Yi, S., McGuire, A. D., Harden, J., Kasischke, E., Manies, K. L., Hinzman, L. D., Liljedahl, A., Randerson, J. T., Liu, H., Romanovsky, V. E., Marchenko, S., and Kim, Y.:

带格式的: 德语(德国)

Interactions between soil thermal and hydrological dynamics in the response of Alaska ecosystems to fire disturbance , J. Geophys. Res., 114, G02015, doi:10.1029/2008JG000841, 2009b.

Yi, S., McGuire, A. D., Kasischke, E., Harden, J., Manies, K. L., Mack, M., and Turetsky, M. R.: A Dynamic organic soil biogeochemical model for simulating the effects of wildfire on soil environmental conditions and carbon dynamics of black spruce forests, J. Geophys. Res., 115, G04015, doi:10.1029/2010JG001302, 2010.

Yi. S., Li, N., Xiang, B., Ye, B. and McGuire, A.D.: Representing the effects of alpine grassland vegetation cover on the simulation of soil thermal dynamics by ecosystem models applied to the Qinghai-Tibetan Plateau, J. Geophys. Res., 118, 1-14, doi: 10.1002/jgrg.20093, 2013.

Yi, S., Wang, X., Qin, Y., Xiang, B., and Ding, Y.: Responses of alpine grassland on Qinghai–Tibetan plateau to climate warming and permafrost degradation: a modeling perspective. Environ. Res. Lett., 9, 074014, doi:10.1088/1748-9326/9/7/074014, 2014a.

Yi, S., Wischnewski, K., Langer, M., Muster, S., Boike, J.: Modeling different freeze/thaw processes in heterogeneous landscapes of the Arctic polygonal tundra using an ecosystem model. Geoscientific Model Development, 7, 1671–1689, 2014b.

Yi S, FragMAP: a tool for long-term and cooperative monitoring and analysis of small-scale habitat fragmentation using an unmanned aerial vehicle, International Journal of Remote Sensing, 38:2686-2697, 2017.

Yin, G., Niu, F., Lin, Z., Luo, J., and Liu, M.: Effects of local factors and climate on permafrost conditions and distribution in Beiluhe basin, Qinghai-Tibet Plateau, China. Science of the Total Environment, 581-582, 472-485, 2017.

Yuan, F. M., Yi, S. H., McGuire, A. D., Johnson, K. D., Liang, J., Harden, J. W., ... and Kurz, W. A.:Assessment of boreal forest historical C dynamics in the Yukon River Basin: relative roles of warming and fire regime change Ecol,Appl., 22, 2091-2109, 2012.

Zhang, Z. F., ~~&~~ and Ward, A. L.: Determining the porosity and saturated hydraulic conductivity of binary mixtures, Vadose Zone J., 10, 313-321, 2011.

Zhuang, Q., V. E. Romanovsky, and A. D. McGuire: Incorporation of a permafrost model into a large-scale ecosystem model: Evaluation of temporal and spatial scaling issues in simulating soil thermal dynamics, J. Geophys. Res., 106(D24), 33649-33670, 2001.

Zhuang, Q., J. Melillo, D. Kicklighter, R. G. Prinn, A. D. McGuire, P. A. Steudler, B. S. Felzer, and S. Hu: Methane fluxes between terrestrial ecosystems and the atmosphere at northern high latitudes during the past century: A retrospective analysis with a process-based biogeochemistry model, Global Biogeochem. Cy., 18, GB3010, doi:10.1029/2004GB002239, 2004.

Zhuang, Q., J. He, Y. Lu, L. Ji, J. Xiao, and T. Luo: Carbon dynamics of terrestrial ecosystems on the Tibetan Plateau during the 20th century: an analysis with a process-based biogeochemical model, Global Ecol. Biogeogr., 19, 649-662, 2010.

Zou, D., L. Zhao, Y. Sheng, J. Chen, G. Hu, T. Wu, J. Wu, C. Xie, X. Wu, Q. Pang, W. Wang, E. Du, W. Li, G. Liu, J. Li, Y. Qin, Y. Qiao, Z. Wang, J. Shi, and G. Cheng: A new map of permafrost distribution on the Tibetan Plateau, The Cryosphere, 11, 2527-2542, 2017.

Table 1. The mean (standard deviation in brackets) of measured soil bulk density, calculated porosity from bulk density, measured porosity of different layers based on soil samples in this study.~~, and particle size diameter fractions （>2 mm means the weight fraction between soil particles greater than 2 mm and total soil sample; while other fraction means the ratio between soil sample weight of a size range and the weight of particles＜2mm） and soil texture (based on USDA classification) of different layers based on soil samples in this study.~~

Layer (cm)	Bulk density (g cm^{-3})	Calculated Porosity (%)	Measured ~~P~~porosity (%)
0—10	1.74（0.21）	34.4（0.08）	28.4（0.03）
10—20	1.81（0.11）	31.8（0.04）	27.7（0.02）
20—30	1.86（0.32）	29.7（0.12）	30.2（0.05）
40—50	1.61（0.23）	39.4（0.09）	29.6（0.02）
70—80	1.62（0.20）	38.8（0.08）	20.6（0.11）
110—120	1.75（0.09）	33.9（0.04）	27.7（0.01）
150—160	1.70（0.15）	36.0（0.06）	26.3（0.02）
190—200	1.81（0.09）	31.6（0.03）	27.1（0.02）

带格式表格

带格式的：字体颜色：自动设置

带格式的：字体颜色：自动设置

带格式的：字体颜色：自动设置

带格式的：字体颜色：自动设置

带格式的：字体颜色：自动设置

带格式的：字体颜色：自动设置

带格式的：字体颜色：自动设置

带格式的：字体颜色：自动设置

Table 2. The particle size diameter fractions （for >2 mm this is the mass ratio between soil particles greater than 2 mm and total soil sample, while for the other fractions this is the ratio between mass of the soil in the size range and the mass of all particles < 2mm） and soil texture (based on USDA classification) of different layers based on soil samples in this study.

Layer (cm)	>2 mm	>63 μ m	2-63 μ m	<2 μ m	Texture
0—10	0.38 （0.07）	0.77 （0.07）	0.18 （0.04）	0.05 （0.02）	Loamy sand
10—20	0.52 （0.14）	0.72 （0.11）	0.20 （0.05）	0.07 （0.05）	Loamy sand
20—30	0.55 （0.17）	0.69 （0.09）	0.24 （0.08）	0.07 （0.01）	Sandy loam
40—50	0.55 （0.19）	0.70 （0.13）	0.26 （0.11）	0.04 （0.02）	Loamy sand
70—80	0.65 （0.16）	0.71 （0.09）	0.25 （0.07）	0.04 （0.02）	Loamy sand
110—120	0.63 （0.05）	0.79 （0.09）	0.19 （0.08）	0.03 （0.02）	Loamy sand
150—160	0.63 （0.09）	0.85 （0.04）	0.13 （0.03）	0.02 （0.01）	Loamy sand
190—200	0.50 （0.19）	0.71 （0.19）	0.24 （0.14）	0.05 （0.05）	Loamy sand

带格式的：英语(英国)

带格式表格

Table 23. The mean (standard deviation in brackets) of the measured frozen and unfrozen dry and saturated soil thermal conductivity (W m^{-1} K^{-1}) of different soil layers.

	Dry		Saturated	
Layer (cm)	Unfrozen	Frozen	Unfrozen	Frozen
0-10	0.238 (0.09)	0.414 (0.09)	2.322 (0.17)	3.122 (0.48)
10~20	0.340 (0.04)	0.365 (0.23)	2.147 (0.47)	3.193 (0.55)
20-30	0.395 (0.07)	0.420 (0.11)	2.743 (0.38)	3.059 (0.29)
40-50	0.346 (0.00)	0.388 (0.14)	2.539 (0.30)	3.184 (0.33)
70-80	0.340 (0.03)	0.289 (0.12)	2.589 (0.16)	3.362 (0.38)
110-120	0.400 (0.06)	0.271 (0.07)	2.616 (0.11)	3.721 (0.05)
150-160	0.401 (0.01)	0.248 (0.07)	2.246 (0.19)	3.647 (0.48)
190-200	0.399 (0.26)	0.392 (0.14)	2.609 (0.12)	3.329 (0.19)

Table 34. The mean (standard deviation) of measured saturated hydraulic conductivity (K_{sat}; mm s^{-1}) and fitted absolute value of saturated matric potential (Ψ_{sat}; mm), fitted pore size distribution parameter (B) and the correlation coefficients (R^2) between calculated matric potential using fitted equations and measured.

	K_{sat}	Matric potential		
Layer (cm)		Ψ_{sat}	B	R^2
0-10	0.0285 (0.0274)	49.14	4.03	0.991
10~20	0.0056 (0.0036)	70.66	4.49	0.996
20-30	0.0047 (0.0027)	27.02	5.22	0.994
40-50	0.0078 (0.0043)	143.4	3.59	0.994
70-80	0.0072 (0.0054)	179.6	3.22	0.993
110-120	0.0315 (0.0054)	603.7	1.89	0.969
150-160	0.0053 (0.0028)	49.17	2.97	0.993
190-200	0.0036 (0.0023)	14.47	4.565	0.989

Table ~~4~~5. Model performance ~~of substituting~~when default sand parameters are substituted with combinations of ~~with~~ measured porosity (I), thermal conductivity (II), hydraulic conductivity (III) and matric potential (IV).

	Best	I+II	I+III	I+IV	II+III	II+IV	III+IV	I+II+III	I+II+IV	I+III+IV	II+III+IV	All
100 cm ST	II											
ALD	I		1									
PLB	II	1	2									
10 cm SM	I	7	2	4				1	5	6		3
40 cm SM	I											
80 cm SM	I	7	1	4				2	6	5		3
160 cm SM	I	1										

Note: Best column ~~showed~~ shows the model simulations (individual parameter substitution) with the smallest root mean squared error (RMSE) for 100 cm soil temperature (ST, °C), active layer depth (ALD, m), permafrost low boundary (PLB, m), 10, 40, 80 and 160 cm soil liquid water content (SM, -); Numbers indicate~~d~~ the combination of parameters ~~(+) had~~ that have smaller RMSE than the best model run using individual parameter substitution. "All" ~~indicated~~ indicates the combination of all 4 parameters. The smallest number ~~indicated~~ indicates the smallest RMSE.

Table ~~5~~ 6 Model performance ~~of~~ when ~~substituting~~ default loam parameters are substituted with combinations of ~~with~~ measured porosity (I), thermal conductivity (II), hydraulic conductivity (III) and matric potential (IV) .

	Best	I+II	I+III	I+IV	II+III	II+IV	III+IV	I+II+III	I+II+IV	I+III+IV	II+III+IV	All
100 cm ST	I	1		2					3			
ALD	I	3	5					1	2	6		4
PLB	II											
10 cm SM	I	7	6	1				5	2	4		3
40 cm SM	I	5	7	1				6	3	4		2
80 cm SM	I											
160 cm SM	I	1	3					2				

Note: Best column ~~showed~~ shows the model simulations (individual parameter substitution) with the smallest root mean squared error (RMSE) for 100 cm soil temperature (ST, °C), active layer depth (ALD, m), permafrost low boundary (PLB, m), 10, 40, 80 and 160 cm soil liquid water content (SM, -); Numbers indicate~~d~~ the combination of parameters ~~(+) had~~ that have smaller RMSE than the best model run using individual parameter substitution. “All” ~~indicated~~ indicates the combination of all 4 parameters. The smallest number ~~indicated~~ indicates the smallest RMSE.

带格式的：英语(美国)
带格式的
带格式的
带格式的
带格式的：英语(美国)
带格式的
带格式的
带格式的
带格式的：英语(美国)
带格式的：英语(美国)
带格式的
带格式的
带格式的
带格式的
带格式的
带格式的
带格式的：英语(美国)
带格式的
带格式的
带格式的
带格式的
带格式的
带格式的
带格式的
带格式的：英语(美国)
带格式的：英语(美国)
带格式的
带格式的
带格式的

Figure 1. a) ~~The location~~Locations of **a)** Beiluhe permafrost station on the Qinghai-Tibetan Plateau, and~~;~~ **b)** the googlemap of the weather station and the surrounding environment.

带格式的: 字体: 加粗

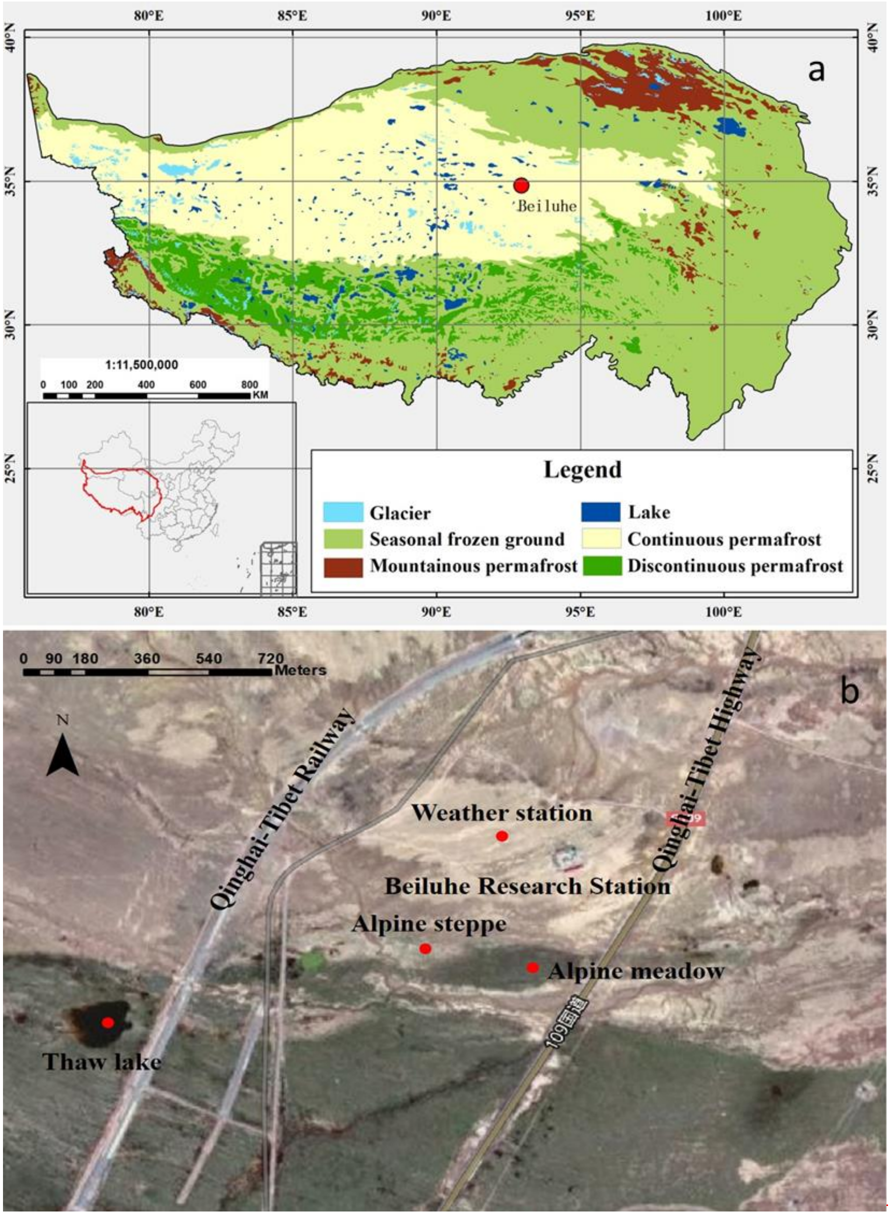
a
80°E
85°E
90°E
95°E
100°E
40°N
35°N
30°N
25°N
Beiluhe
1:11,500,000
0 100 200 400 600 800 KM
Legend
Glacier
Lake
Seasonal frozen ground
Continuous permafrost
Mountainous permafrost
Discontinuous permafrost
b
0 90 180 360 540 720 Meters
N
Qinghai-Tibet Railway
Qinghai-Tibet Highway
Weather station
Beiluhe Research Station
Alpine steppe
Alpine meadow
Thaw lake

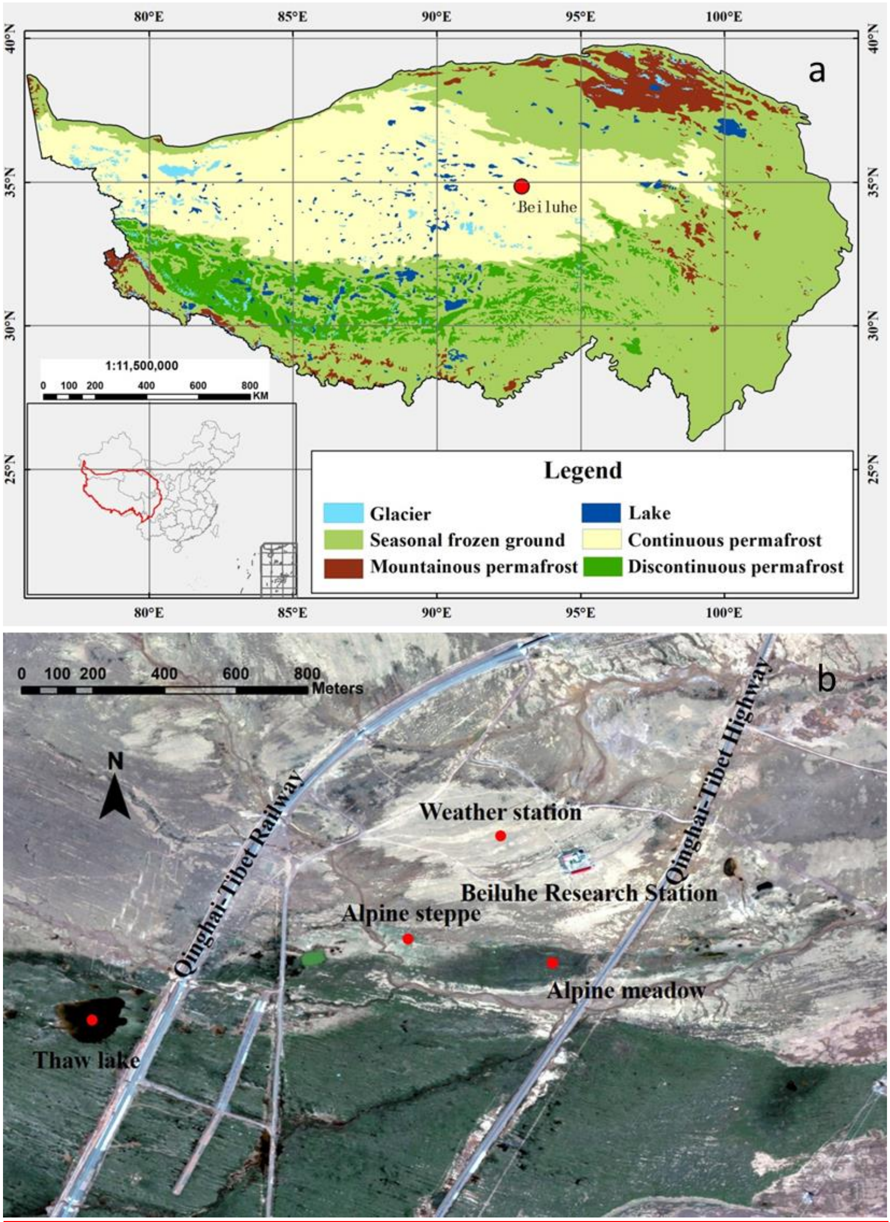
a
80°E
85°E
90°E
95°E
100°E
40°N
35°N
30°N
25°N
Beiluhe
1:11,500,000
0 100 200 400 600 800
KM
Legend
Glacier
Lake
Seasonal frozen ground
Continuous permafrost
Mountainous permafrost
Discontinuous permafrost
b
0 100 200 400 600 800
Meters
N
Qinghai-Tibet Railway
Qinghai-Tibet Highway
Weather station
Beiluhe Research Station
Alpine steppe
Alpine meadow
Thaw lake

Figure 2. Images of site conditions: **a)** the aerial view of the weather station and the excavated soil pit (the borehole is located in the lower left corner of white fence); **b)** the detailed view of the excavated soil pit; and **c)-e)** examples of vegetation, gravel and stones (iron frame is about 0.5 m×0.5 m).

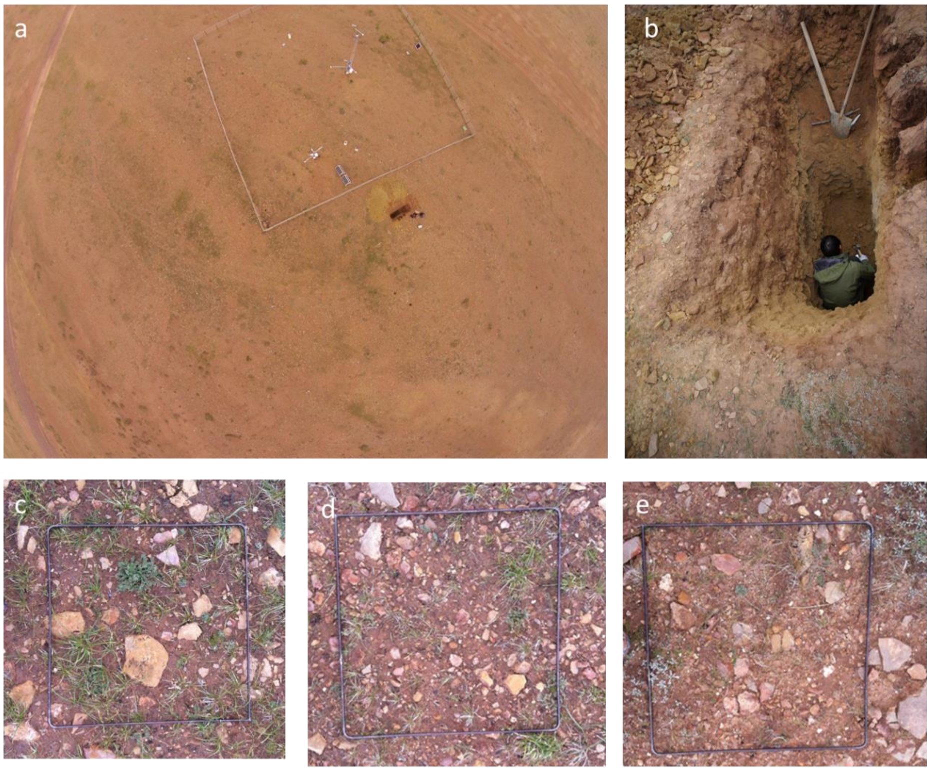

带格式的：字体：加粗
带格式的：字体：加粗
带格式的：字体：加粗
带格式的：字体：加粗
带格式的：字体：加粗

Figure 3. Time series of data measured at the Beiluhe weather station, Qinghai-Tibetan Plateau, 2003 to 2011: **a)** air temperature (TA, ^{o}C); **b)** downward solar radiation (R, W m^{-2} w/m^{2}); **c)** precipitation (PREC, mm) and **d)** relative humidity (RH, %) measured on Beiluhe weather station on the Qinghai-Tibet Plateau from 2003 to 2011.

带格式的：字体：加粗

带格式的：字体：加粗

带格式的：字体：加粗

带格式的：上标

带格式的：字体：加粗

带格式的：字体：加粗

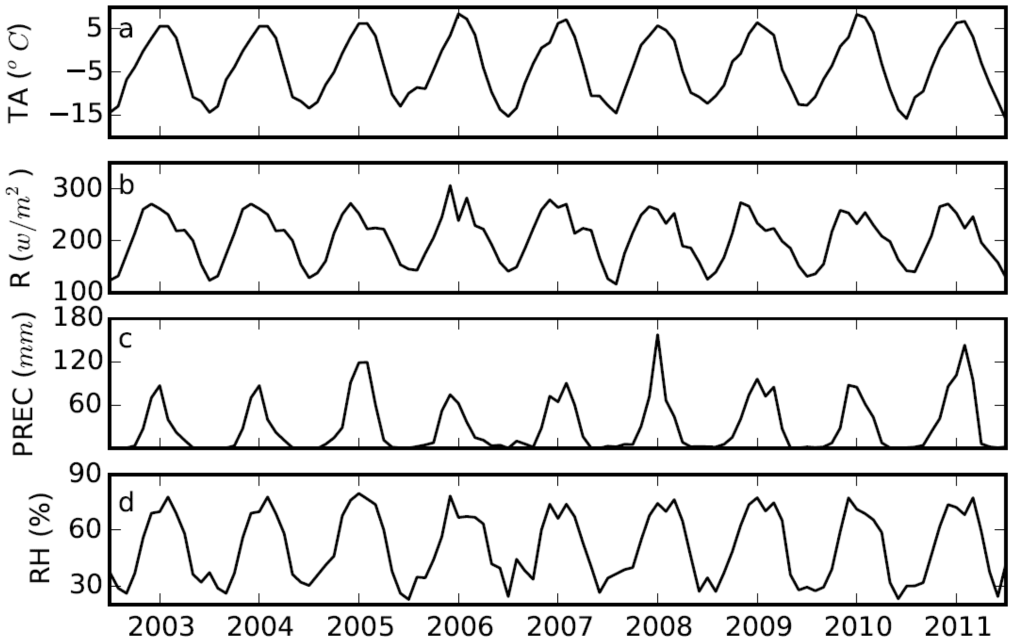

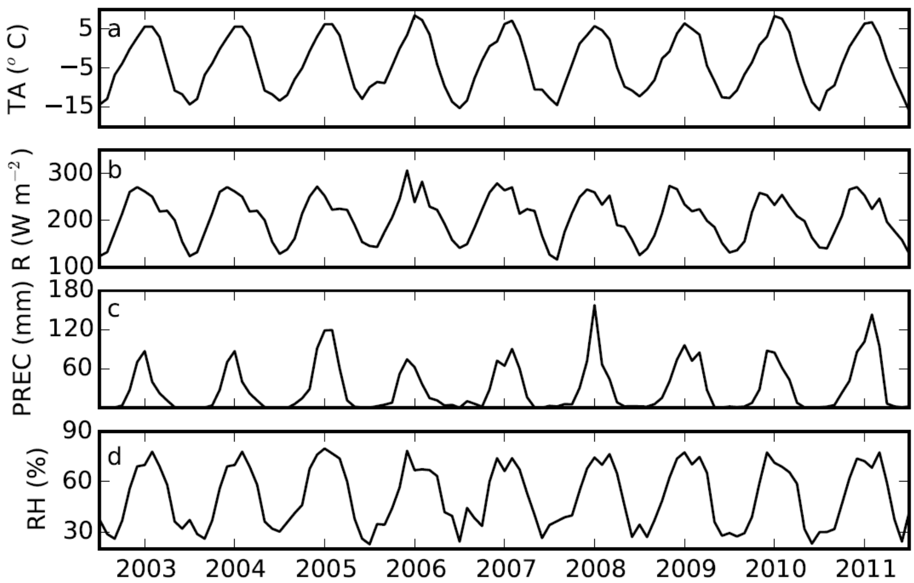

Figure 4. The relationship between soil wetness (solid and dotted lines represent frozen and unfrozen cases) and soil thermal conductivity (W m^{-1} K^{-1}) from: **a)** measured values (Measured; dots and empty diamonds represent measured frozen and unfrozen soil thermal conductivities, respectively), **b)** using the Côté and ~~Konard~~Konrad (2005) scheme (CK); and **c)** using the Farouki (1986) scheme (Farouki). Thick and thin lines represent relationships for sand and loam, respectively.

带格式的：上标

带格式的：上标

1 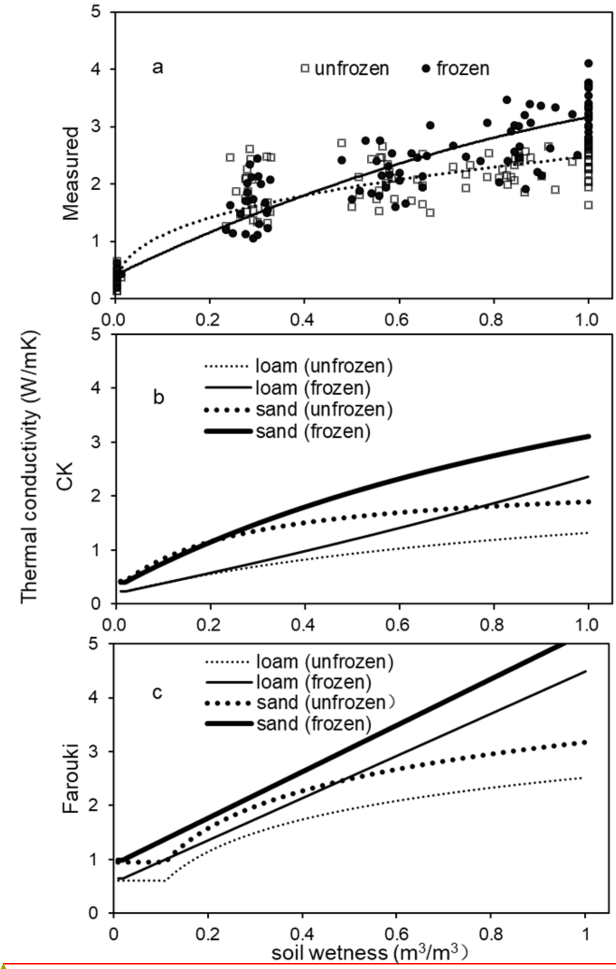

带格式的：字体颜色：红色

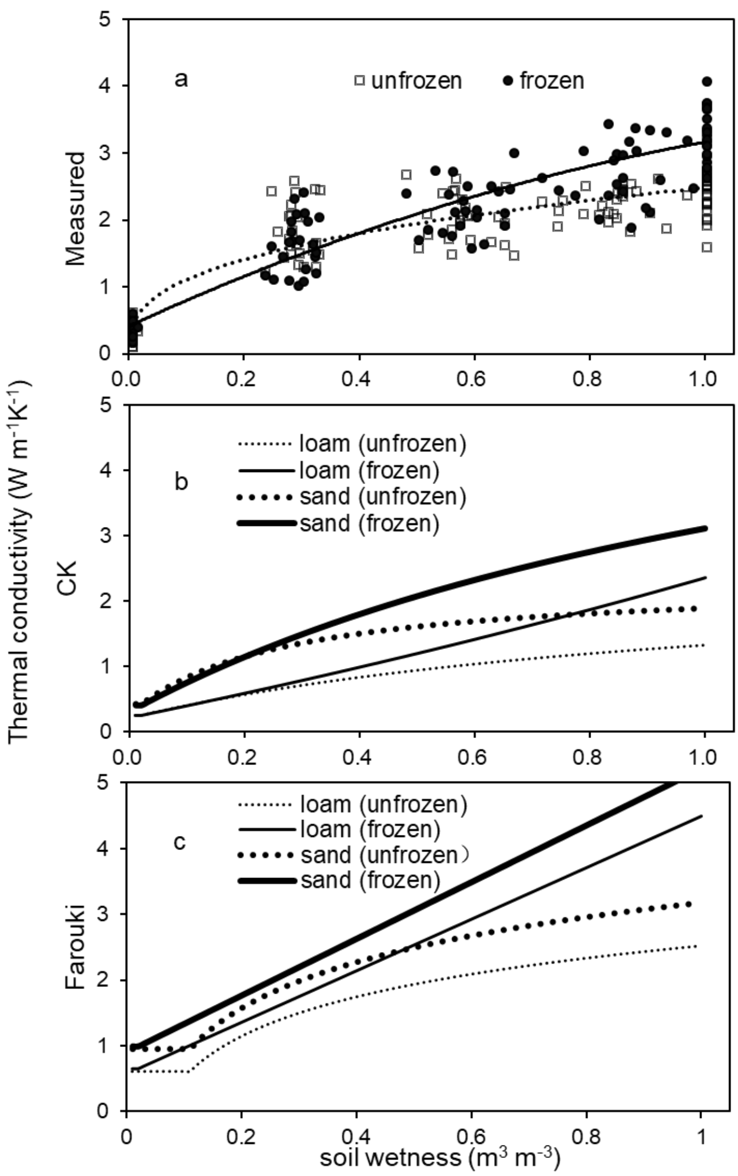
Thermal conductivity (W m-1K-1)
a
unfrozen
frozen
Measured
b
loam (unfrozen)
loam (frozen)
sand (unfrozen)
sand (frozen)
CK
c
loam (unfrozen)
loam (frozen)
sand (unfrozen)
sand (frozen)
Farouki
soil wetness (m3 m-3)

Figure 5.The relations between **a)** ~~the relationship between~~ saturated hydraulic conductivity (mm s^{-1}) and coarse fragement fraction (Solid dots represent measured value; empty circle and empty triangle represent the corresponding values of sand and loam used in Community Land Model, respectively)~~;~~ , and **b)** ~~the relationship between~~ soil wetness (lines) and absolute value of matric potential (mm H_2O) at three representative depths (~~.~~ ~~Solid~~ solid and dashed lines represent default values (Oleson et al., 2010) of sand and loam, respectively ~~(Oleson et al., 2010~~).

带格式的: 字体颜色: 红色

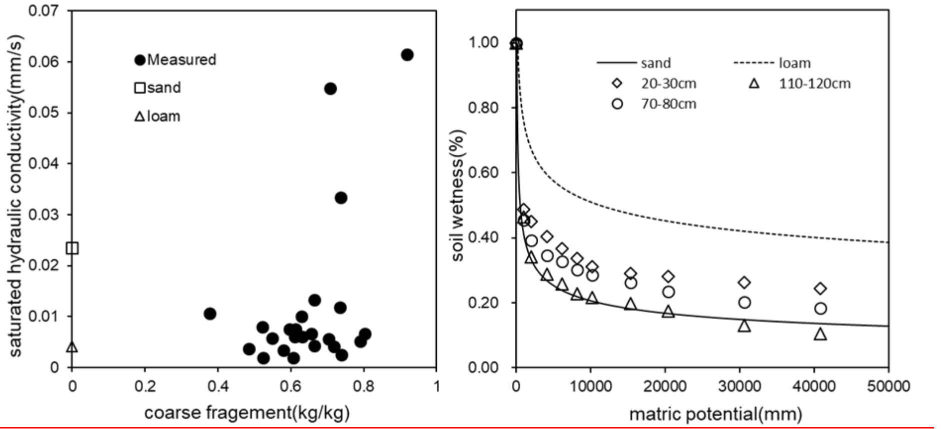

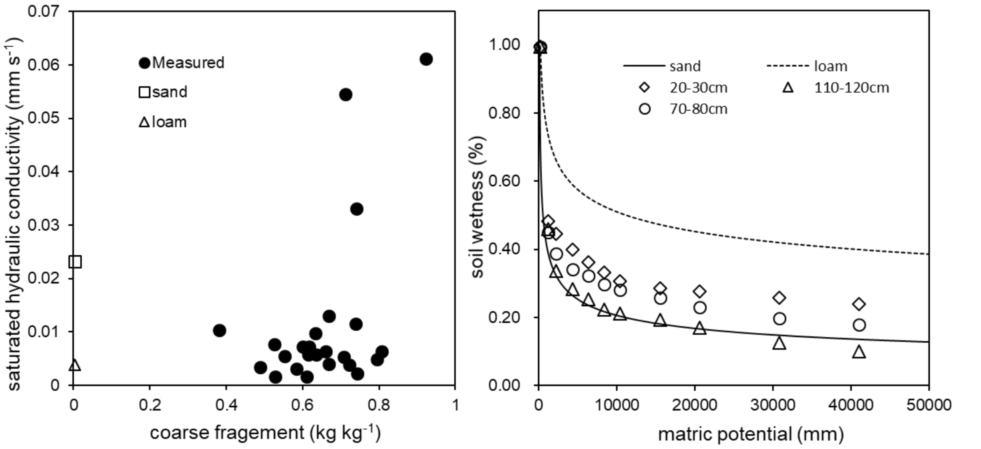

Figure 6. Comparisons of soil temperatures simulated using default parameters of for sand, loam, and our measured parameters (lines) with measured soil temperatures (dots) at 20, 100, 200 and 400 cm depths. Error bars showed the standard deviations calculated based on 9 simulations with 3 different slopes and 3 different soil thicknesses.

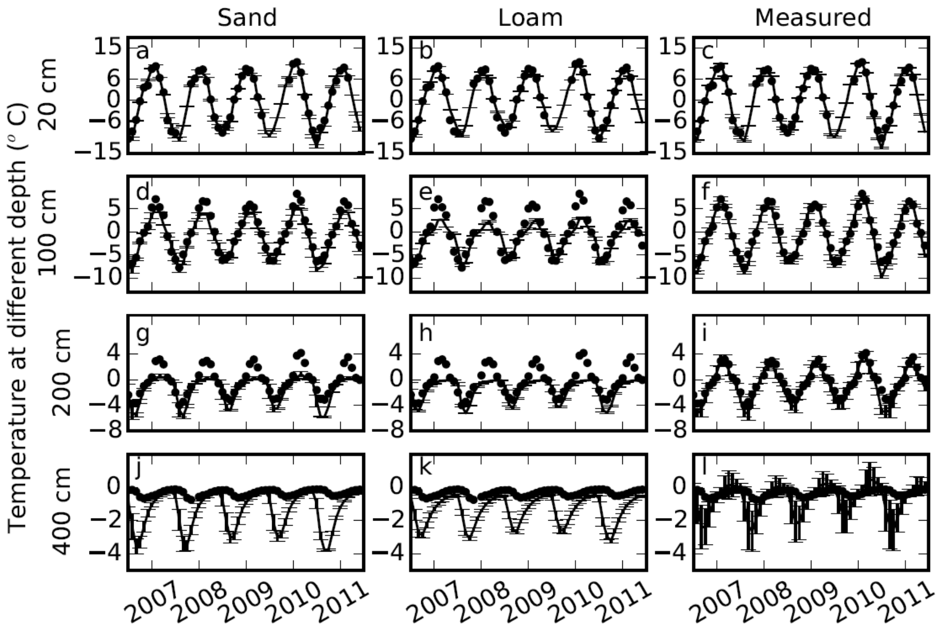
Sand
Loam
Measured
Temperature at different depth (° C)
20 cm
100 cm
200 cm
400 cm
a
b
c
d
e
f
g
h
i
j
k
l
2007
2008
2009
2010
2011

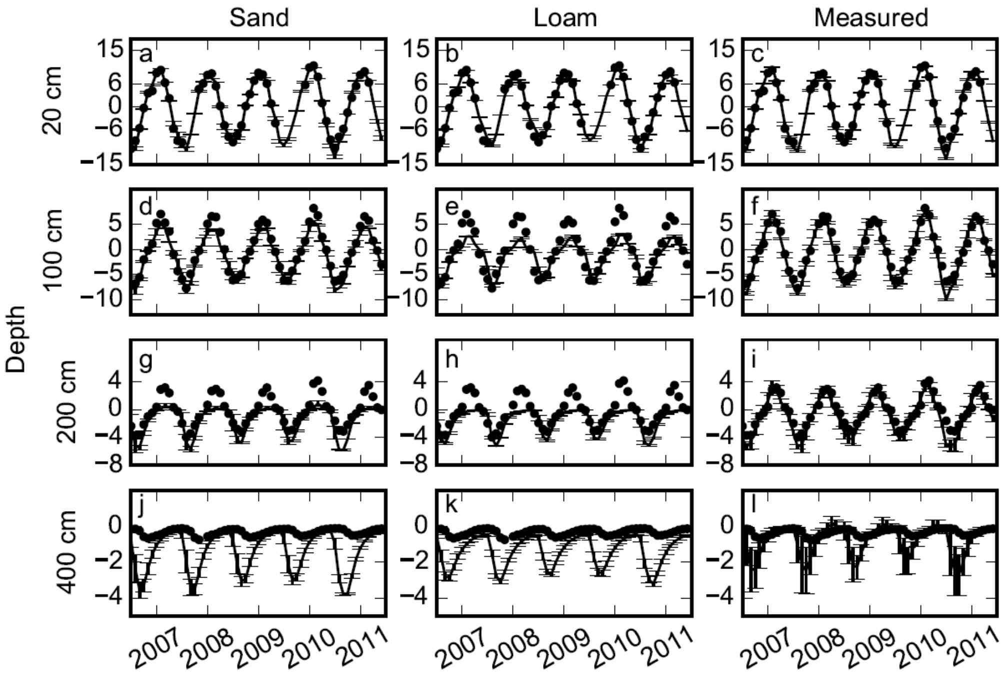
Sand
Loam
Measured
Depth
20 cm
100 cm
200 cm
400 cm
a
b
c
d
e
f
g
h
i
j
k
l
2007
2008
2009
2010
2011

Figure 7. Comparisons of soil volumetric liquid water content (VWC) simulated using default parameters sand, default loam, and measured parameters (lines) with measured soil moistures (dots) at 10, 40, 80 and 160 cm depths. Error bars showed the standard deviation calculated based on 9 simulations with 3 different slopes and 3 different soil thicknesses.

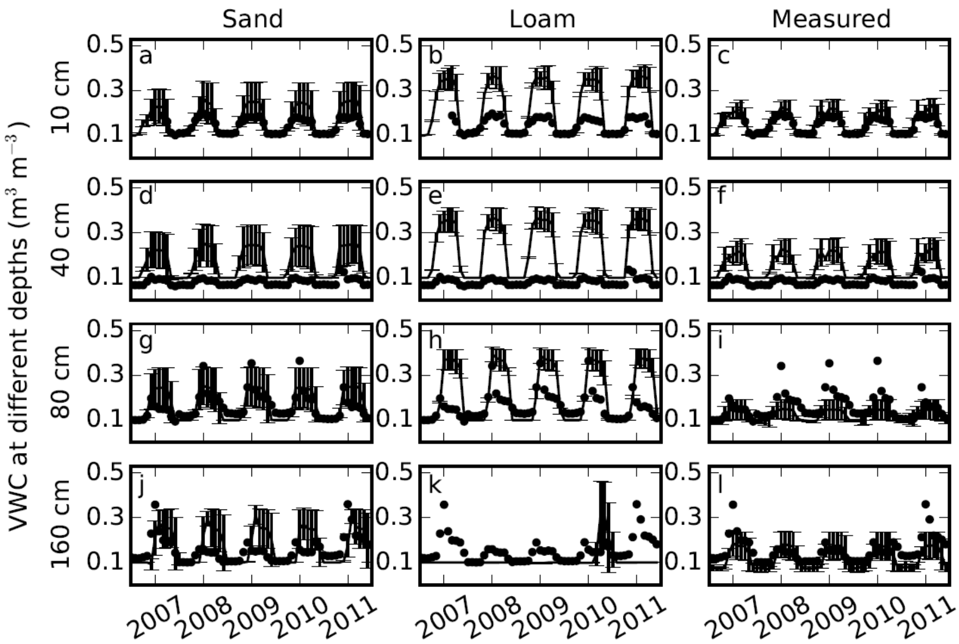

Sand
Loam
Measured
VWC at different depths (m^3 m^{-3})
10 cm
40 cm
80 cm
160 cm
0.5
0.3
0.1
a b c d e f g h i j k l
2007 2008 2009 2010 2011

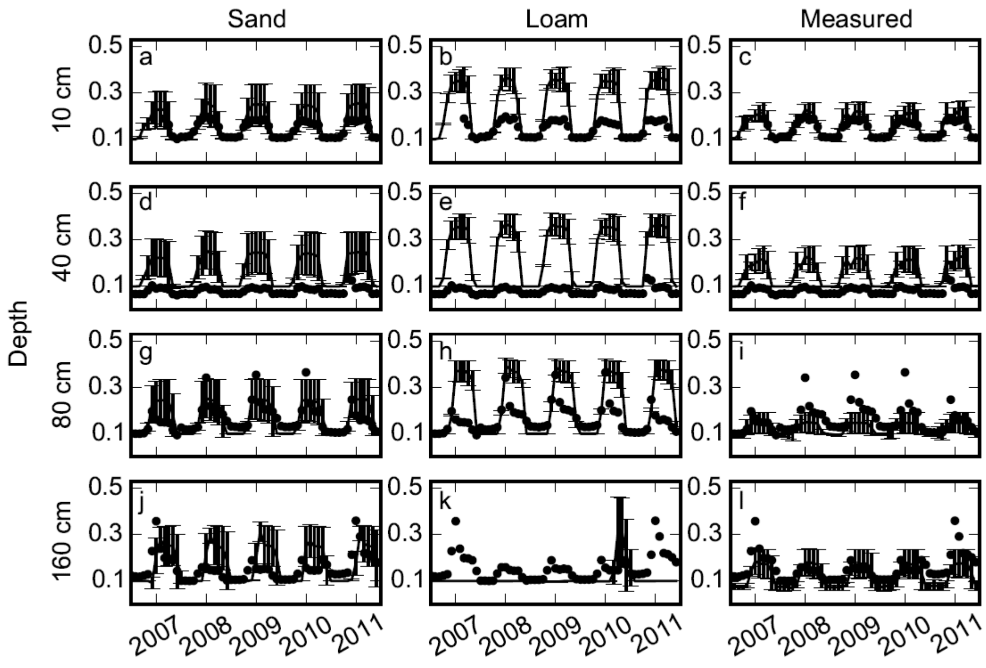

Sand
Loam
Measured
Depth
10 cm
40 cm
80 cm
160 cm
0.5
0.3
0.1
a b c d e f g h i j k l
2007 2008 2009 2010 2011

带格式的: 字体颜色: 红色

Figure 8. Contour plots showing **a)** ~~Contours of measured~~ soil temperature (^{o}C) from borehole measurements down to 5 m ~~and~~ superimposed with simulated active layer depths over the period of 2003-2011; and **b)** ~~same as a) but~~ground temperature down to 50 m ~~and for~~superimposed with the simulated permafrost low boundary. Black, blue and magenta represent simulations with loam, sand and measured parameters, respectively. Error bars show the standard deviation calculated based on 9 simulations with 3 different slopes and 3 different soil thicknesses.

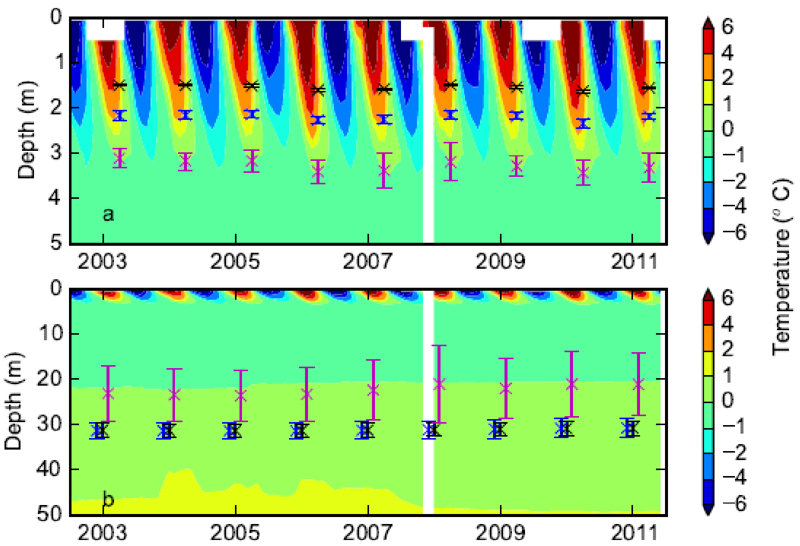

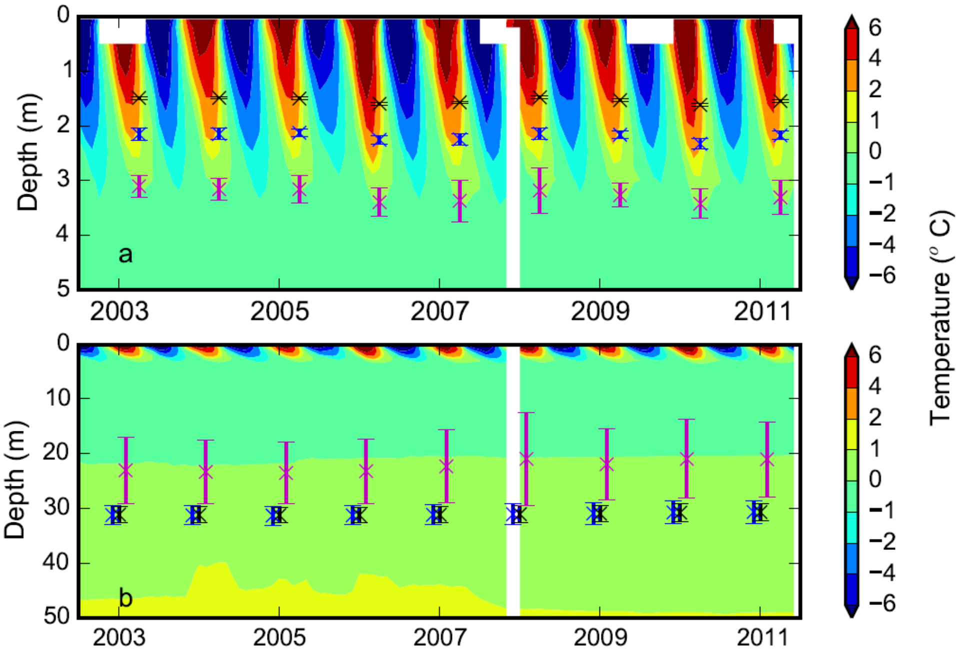
Depth (m)
0
1
2
3
4
5
a
2003
2005
2007
2009
2011
6
4
2
1
0
−1
−2
−4
−6
Temperature (o C)
Depth (m)
0
10
20
30
40
50
b
2003
2005
2007
2009
2011
6
4
2
1
0
−1
−2
−4
−6

带格式的：字体颜色：红色

Figure 9. –Root mean squared errors between measurements and model simulations (with different combinations of measured porosity (I), thermal conductivity (II), hydraulic conductivity (III) and matric potential (IV) of default sand parameters) for **a)** 20 and **b)** 100 cm soil temperatures (^{o}C), **c)** active layer depth (ALD, m) and **d)** permafrost low boundary (PLB, m). O and All represent model runs without substitution of default parameters and with all 4 parameters substituted, respectively. Mean and standard deviation of model simulations with 3 different soil thicknesses at each slope (slope 0: 0^{o}; slope 5: 5^{o}; slope 10: , and 10^{o}) are shown.

带格式的: 字体: 加粗

带格式的: 字体: 加粗

带格式的: 字体: 加粗

带格式的: 字体: 加粗

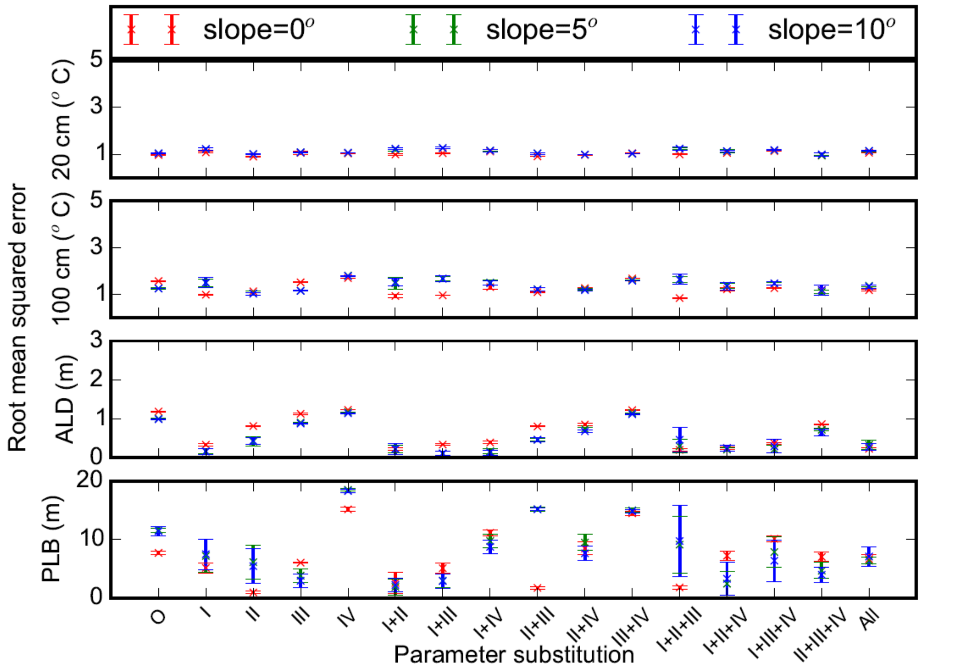

1 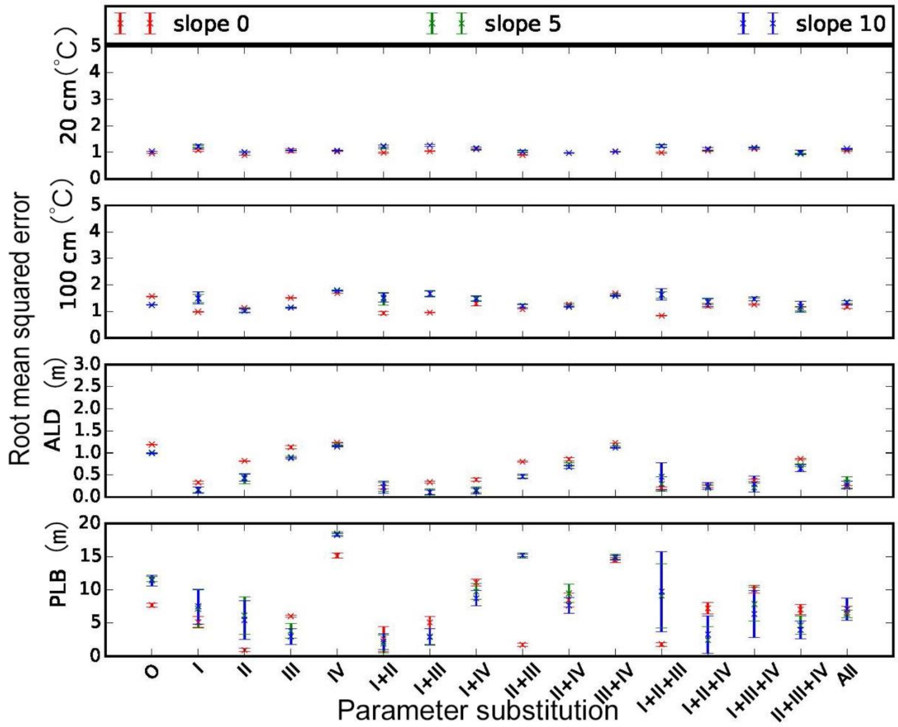

2

带格式的：字体颜色：红色

Figure 10. Root mean squared errors between measurements and model simulations (with different combinations of measured porosity (I), thermal conductivity (II), hydraulic conductivity (III) and matric potential (IV) of default loam parameters) for **a)** 20 and **b)** 100 cm soil temperatures (^{o}C), **c)** active layer depth (ALD, m) and **d)** permafrost low boundary (PLB, m). O and All represent model runs without substitution of default parameters and with all 4 parameters substituted, respectively. Mean and standard deviation of model simulations with 3 different soil thicknesses at each slope (slope 0: 0^{o};, slope 5: 5^{o};, andslope 10: 10^{o}) are shown.

带格式的：字体：加粗

带格式的：字体：加粗

带格式的：字体：加粗

带格式的：字体：加粗

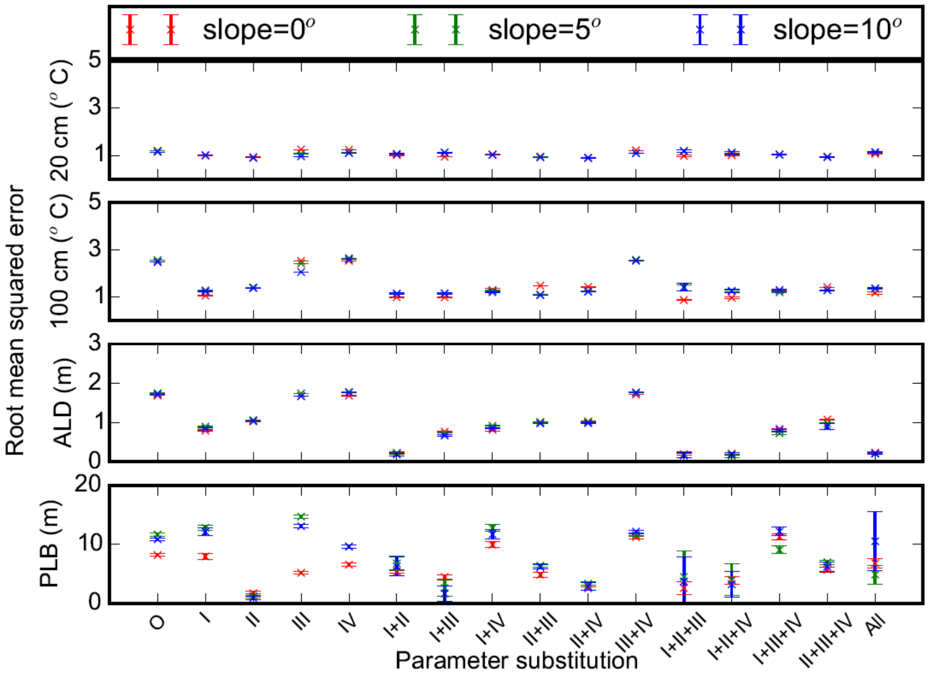

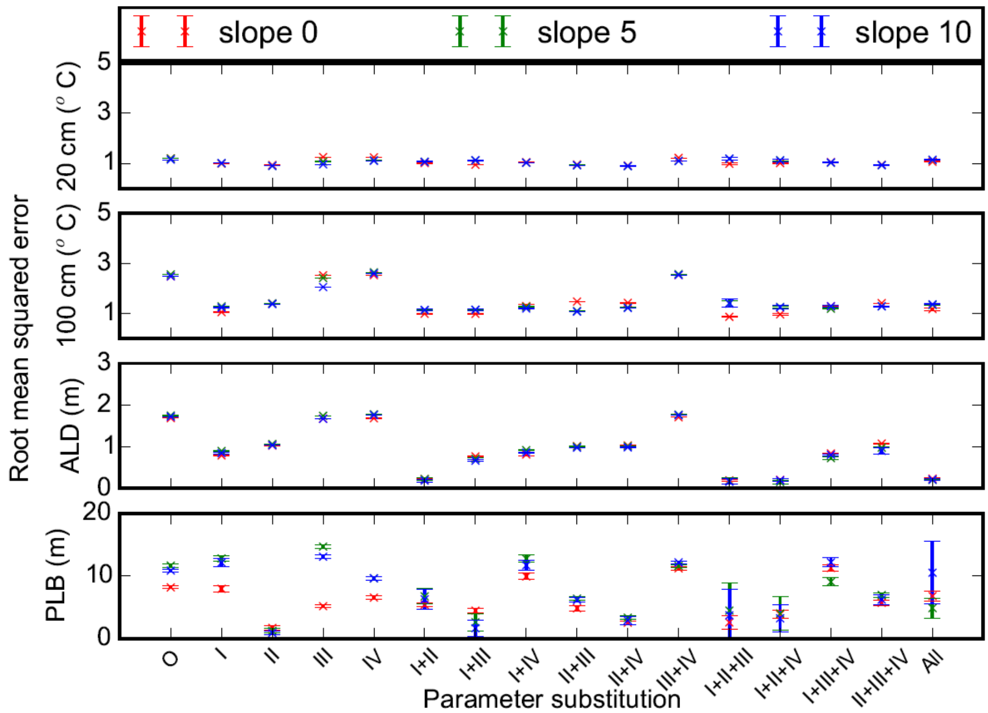
slope 0
slope 5
slope 10
Root mean squared error
20 cm (° C)
100 cm (° C)
ALD (m)
PLB (m)
O
I
II
III
IV
I+II
I+III
I+IV
II+III
II+IV
III+IV
I+II+III
I+II+IV
I+III+IV
II+III+IV
All
Parameter substitution

带格式的：字体颜色：红色

Figure 11. Root mean squared errors between measurements and model simulations (with different combinations of measured porosity (I), thermal conductivity (II), hydraulic conductivity (III) and matric potential (IV) of default sand parameters) for ~~a)~~ 10 cm, ~~b)~~ 40 cm, ~~c)~~ 80 cm and ~~d)~~ 160 cm soil volumetric liquid water content. O and All represent model runs without substitution of default parameters and with all 4 parameters substituted, respectively. Mean and standard deviation of model simulations with 3 different soil thicknesses at each slope (~~slope 0:~~ 0°~~; slope 5:~~ , 5°~~; slope 10:~~ , and 10°) are shown.

带格式的: 字体: 加粗

带格式的: 字体: 加粗

带格式的: 字体: 加粗

带格式的: 字体: 加粗

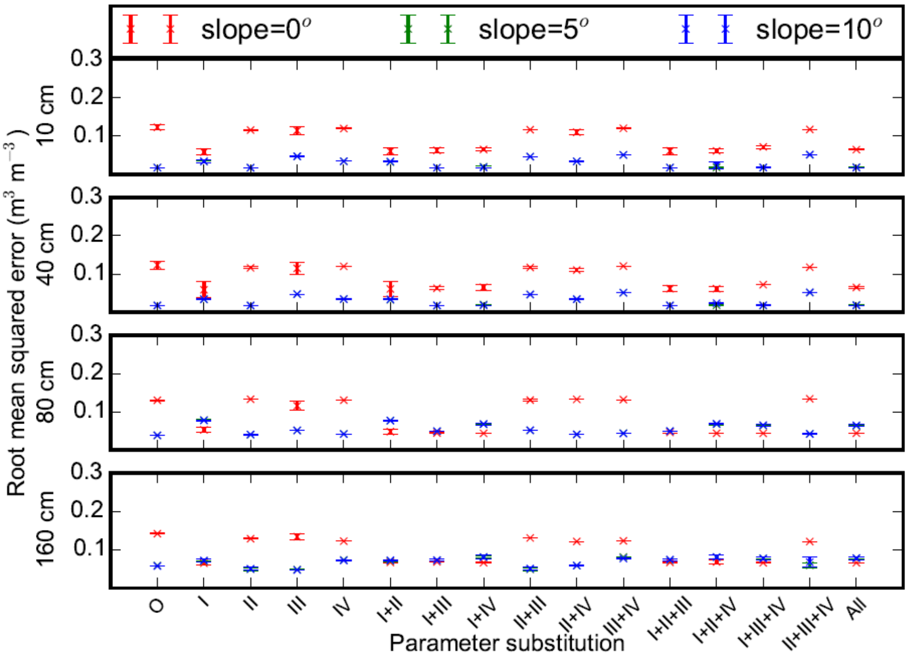

Figure 12. Root mean squared errors between measurements and model simulations (with different combinations of measured porosity (I), thermal conductivity (II), hydraulic conductivity (III) and matric potential (IV) of default loam parameters) for a) 10 cm, b) 40 cm, c) 80 cm and d) 160 cm soil volumetric liquid water content. O and All represent model runs without substitution of default parameters and with all 4 parameters substituted, respectively. Mean and standard deviation of model simulations with 3 different soil thicknesses at each slope (slope 0: 0^{o}; slope 5:, 5^{o}; slope 10:, and 10^{o}) are shown.

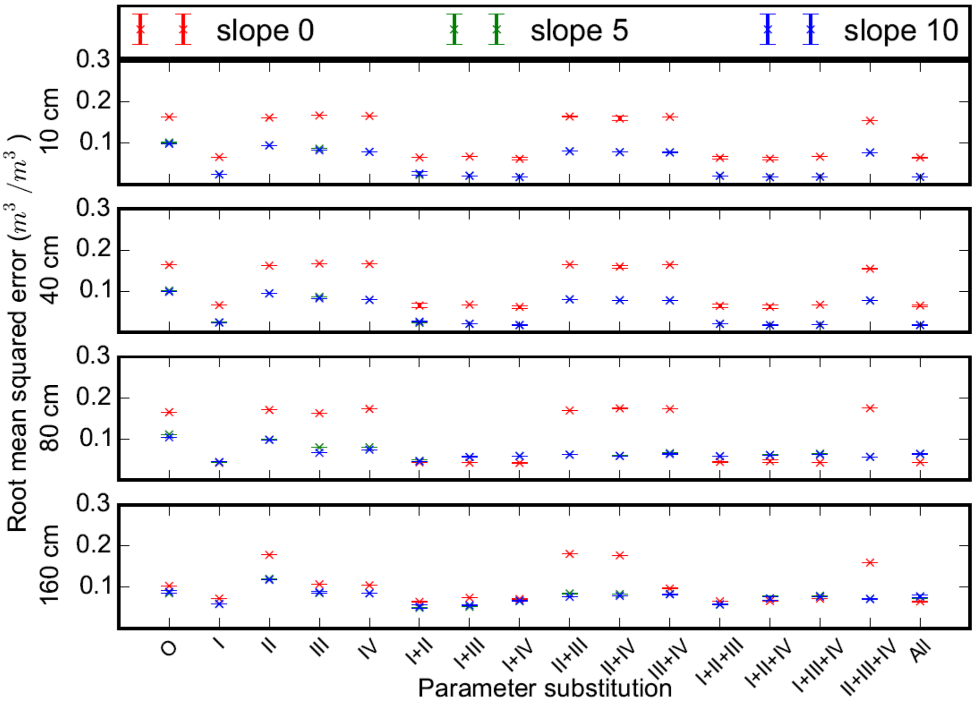

带格式的：字体：加粗
带格式的：字体：加粗
带格式的：字体：加粗
带格式的：字体：加粗
带格式的：字体颜色：红色

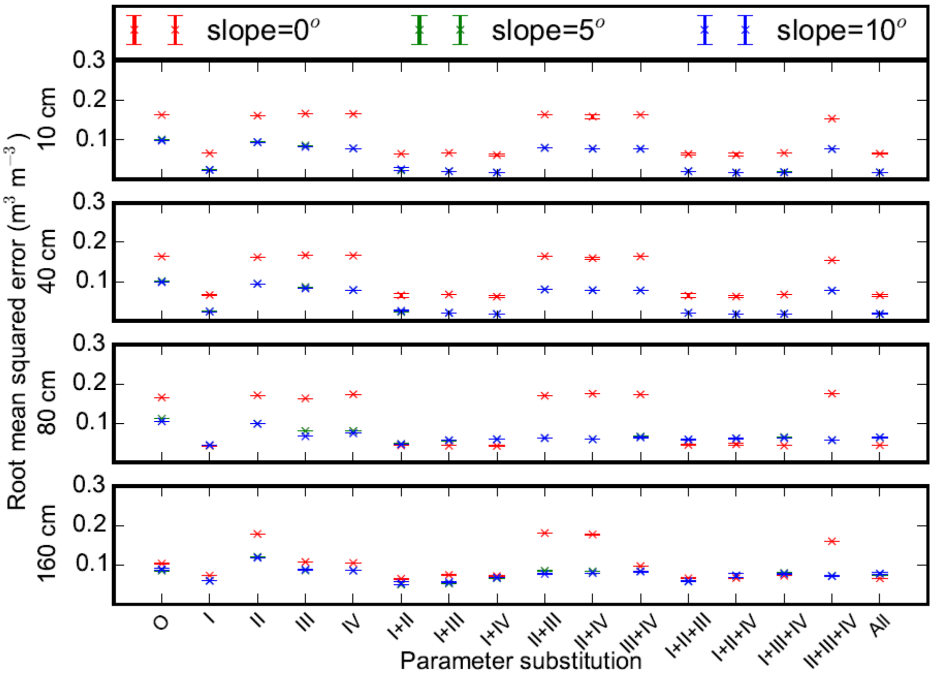

slope=0°
slope=5°
slope=10°
Root mean squared error (m^3 m^{-3})
10 cm
40 cm
80 cm
160 cm
0.3
0.2
0.1
O
I
II
III
IV
I+II
I+III
I+IV
II+III
II+IV
III+IV
I+II+III
I+II+IV
I+III+IV
II+III+IV
All
Parameter substitution